UNIVERSITY OF CALIFORNIA

Santa Barbara

Microbial Oxidation of Marine Hydrocarbons: Quantifying Rates of Methane, Ethane, Propane, and Butane Consumption

A dissertation submitted in partial satisfaction of the

requirements for the degree Doctor of Philosophy

in Earth Science

by

Stephanie Diana Mendes

Committee in charge:

Professor David L. Valentine, Chair

Professor Jordan Clark

Professor Craig Carlson

March 2015

The dissertation of Stephanie Diana Mendes is approved.

_____

Jordan F. Clark

_____

Craig Carlson

_____

David L. Valentine, Committee Chair

March 2015

Microbial Oxidation of Marine Hydrocarbons: Quantifying Rates of Methane, Ethane, Propane, and Butane Consumption

by

Stephanie D. Mendes

VITA OF STEPHANIE D. MENDES
March 2015

EDUCATION

Bachelor of Science in Chemistry, California State University, Chico, May 2009
Doctor of Philosophy in Earth Science, University of California, Santa Barbara, December 2014 (expected)

PROFESSIONAL EMPLOYMENT

Fall 2013: Adjunct Professor, Department of Earth Science, Santa Barbara City College
Summer 2013: Summer Teaching Associate, University of California, Santa Barbara
2009-2014: Outreach Coordinator, Center for Science and Engineering Partnerships (CSEP), University of California, Santa Barbara

PUBLICATIONS

M. Du, S. Yvon-Lewis, F. Garcia-Tigreros, D. Valentine, **S. Mendes**, J. Kessler, "High resolution measurements of methane and carbon dioxide at a natural seep reveal dynamics of air-sea flux" Environmental Science and Technology. (in review)

L. Cárdenas, D. Garbe-Schönberg, J. Sellanes, I. Melville, **S. Mendes**, P. Muñoz, "Geochemistry of pore water trace metals from different reducing systems associated with benthic chemosynthetic activity at the SE Pacific margin off Chile" Progress in Oceanography. (in review)

D. Valentine, J. Kessler, M. Redmond, **S. Mendes**, M. Heintz, C. Farwell, L. Hu, F. Kinnaman, S. Yvon-Lewis, M. Du, E. Chan, F. Garcia Tigreros, C. Villanueva "Propane respiration jump-starts microbial response to a deep oil spill" Science 330 (6001), 208, October 08, 2010

J. Kessler, D. Valentine, M. Redmond, M. Du, E. Chan, **S. Mendes**, E. Quiroz, C. Villanueva, S. Shusta, L. Werra, S. Yvon-Lewis, T. Weber. "A persistent oxygen anomaly reveals the fate of spilled methane in the deep Gulf of Mexico" Science 331 (6015), 312-315, January 06, 2011

RECENT AWARDS

2011-2014 National Research Council- Ford Foundation Pre-Doctoral Fellowship (3 year Fellowship)
2009-11 National Science Foundation- Louis Stokes Bridges to the Doctorate (2 year Fellowship)

ABSTRACT

Microbial Oxidation of Marine Hydrocarbons: Quantifying Rates of Methane, Ethane, Propane, and Butane Consumption

by

Stephanie Diana Mendes

Natural gases have many environmental consequences if released into the atmosphere due to their high global warming potentials. However, these gases are subject to oxidation by microorganisms, which act as an effective biofilter that limits the atmospheric input. Organisms responsible for this oxidation are present in a wide range of environments and hydrocarbon compositions. To quantify the rate at which a microbial community oxidizes and regulates the flux of hydrocarbons into an environment, a combination of chemical tracer techniques is typically applied. This work applied both stable and radioactive tracers to monitor the oxidation capacity of the microbial community in both water column and marine sediment, with hydrocarbon concentrations generally ranging from low (coastal systems near hydrocarbon reservoirs) to medium (natural seeps) to high (oil spills).

Samples containing low and medium natural gas concentrations were collected from the world's largest natural marine seep field, Coal Oil Point, located offshore of Santa Barbara, California. Natural gas emanating from Coal Oil Point first diffuses into sediment porewater before migrating into the overlying water column to form a dissolved plume. Novel

radioactive tracers were developed and applied to assess the timing by which microbes metabolize these gases within both the water column and sediment. A three phase study was employed to track the dissolved hydrocarbon plume within the water column. Phase 1 synthesized tritiated ethane, propane, and butane using Grignard reagents and tritiated water; Phase 2 systematically assessed the experimental conditions, wherein the indigenous microbial community was found to rapidly oxidize ethane, propane, and butane; Phase 3 applied radioactive tracers to track microbial oxidation within a dissolved hydrocarbon plume. Spatial and temporal patterns of ethane, propane, and butane oxidation down current from the hydrocarbon seeps demonstrated that >99% of these gases were metabolized within 1.3 days following initial exposure. Estimates based on the observed metabolic rates and carbon mass balance calculations suggest that ethane-, propane-, and butane-consuming microorganisms may transiently account for a majority of the total microbial community within impacted waters.

Sediment studies focused on the metabolism of ethane oxidation from two individual seeps within the Coal Oil Point field: Campus Point Mounds and Patch Seep. Ethane oxidation was quantified in slurry incubations under anaerobic conditions, which indicated that >97% of the gas was removed after 43 days when incubated near *in situ* temperature and gas concentrations. This study was the first to quantify anaerobic ethane oxidation within cold seep sediments. Total ethane consumption rates from Campus Point Mounds and Patch Seep were calculated to be 2 μM day^{-1} and 0.012 μM day^{-1}, respectively, revealing that anaerobic oxidation in sediment is a dynamic process capable of modulating ethane's release into the ocean and atmosphere. Ethane oxidation was also quantified in whole core

profiles. These profiles showed elevated ethane oxidation rates to depths of 11 cm beneath the sea floor, but rates below detection in the underlying zone of low sulfate.

Samples containing high natural gas concentrations were collected from the Deepwater Horizon oil spill, both during and following the nearly three-month hydrocarbon release. Microbial oxidation of ethane and propane was tracked using stable isotope (^{13}C) tracers. Within 20 weeks of the onset of hydrocarbon release, the microbial communities had "bloomed" to consume elevated concentrations of ethane and propane, and subsequently "busted" following a prolonged period of starvation. This short time interval for complete natural gas consumption contradicts initial predictions based on previous methane studies, and indicates that oxidation rates can accelerate in environments of high hydrocarbon concentrations.

TABLE OF CONTENTS

I. Introduction

Natural gas and oil, along with other hydrocarbons, are produced in Earth's subsurface with pressure and time. Organic matter, dominantly marine phytoplankton once living in the upper water column, is deposited on the sea floor and buried along with sediment. Geothermal heat then transforms the organic matter into hydrocarbons. These processes occur over geologic time, typically on the order of millions of years. Natural gas and oil are less dense than water. They migrate upward toward the surface unless obstructed by an impermeable barrier (often a fine-grained sedimentary rock such as shale). Natural seeps form at the surface in the absence of a barrier or the presence of a conduit like a fault. A significant amount of the total natural gas emission to the atmosphere is from natural seeps, with over 10,000 known throughout the globe (Figure 1) (Etiope and Ciccioli 2009). However, gas and oil from subsurface reservoirs can also reach the surface if released from anthropogenic extraction (Coast Guard 2013).

Natural gas seeps are composed of primarily methane (C1), ethane (C2), propane (C3), and butane (C4). These gases pose significant environmental repercussions if released in large quantities into the ocean and atmosphere. Methane is the most abundant and the most potent as a greenhouse gas, and thus has received more attention than its longer chain analogs (Etiope et al. 2008, Cicerone and Oremland 1988, Fung et al. 1991); however, ethane, propane, and butane also impact Earth's climate and atmospheric chemistry (Etiope and Ciccioli 2009, Pozzer et al. 2010).

According to Reeburgh (2007), an estimated 75-310 Tg of methane is produced annually in the Ocean's subsurface, but only ~10 Tg of that methane makes it to the atmosphere. Marine microorganisms living in the water column and sediment act as an effective biofilter (Reeburgh 2007). Aerobic methane consumers have been studied since the early 20th century, when Sohngen (1906) recognized that methane was produced in large amounts and suggested that the low atmospheric concentrations of this gas were due to its oxidation by microbes. Sohngen's study also led to the identification of the first methane oxidizing bacterium, *Bacillus methanicus*. Since then, methanotrophs (methane consuming organisms) have been identified in a variety of environments, both terrestrial and marine (Bartlett and Harriss 1993, Reeburgh 2007).

The oxidation of methane also occurs in anaerobic environments, but the microbial community responsible is fundamentally different. Anaerobic methane consumers, coupled with sulfate-reducing bacteria, survive independent of photosynthesis and produce high concentrations of hydrogen sulfide and carbon dioxide in anoxic zones of marine sediments (Levin 2005). Even though methane is the most abundant natural gas released in these environments, its longer chain analogs are also consumed by the microbial community. Similarly to methane, the atmospheric reservoir for ethane, propane, and butane is only a fraction of the total estimated emission (Plassdulmer et al. 1995) (Figure 2). While evidence for microbial consumption of ethane, propane, and butane has also been observed by a handful of studies in both oxic and anoxic settings (Kniemeyer et al. 2007; Redmond, Valentine and Sessions 2010; Perry 1979; Sassen et al. 2004; Kinnaman, Valentine and

Tyler 2007; Head, Jones and Roling 2006; Rojo 2009, Valentine et al. 2010), far less is still known about consumption of these non-methane hydrocarbon gases.

Aerobic hydrocarbon oxidizing bacteria are typically divided into at least four broad groups based on substrate specificity: i) methane oxidizers; ii) ethane, propane, and butane oxidizers; iii) longer chain alkane (≥C5) oxidizers; and iv) polycyclic aromatic hydrocarbon (PAH) oxidizers (van Beilen et al. 2002). Organisms that consume methane are typically limited to one carbon substrates (Hanson and Hanson 1996), and thus do not readily contribute to the oxidation of non-methane hydrocarbons. Organisms that consume n-alkanes include numerous metabolic generalists as well as obligate alkane degraders such as *Alcanivorax*. Organisms that consume PAHs tend to also be specialists, such as *Cycloclasticus*. However, the biochemistry of ethane, propane and butane consuming organisms are largely unknown in marine environments, and the consumers may include obligate ethanotrophs (Redmond et al., 2010) and generalist alkane degraders (Redmond and Valentine 2012).

Hydrocarbon consuming communities are typically a complex mixture of microbial populations and the role of natural gas in these ecosystems is not well established. The rate by which natural gas fluctuates through a system is a reflection of the entire microbial community's population and metabolic capacity. Biogeochemical tracers, both natural and artificial, can be applied to quantify this rate. Reeburgh et al. (1991) first used tritium labeled methane to calculate microbial oxidation as the major sink of methane in some aquatic environments. Radiolabeled methane minimizes perturbation to the natural system while allowing for rapid analysis following sample collection (~12-24 hours). Since then,

many studies have adapted and built on tracer methods to assess microbial consumption of methane (Valentine et al. 2001, Heintz 2012).

The work presented in this dissertation introduces a novel method with tritium labeled ethane, propane, and butane to quantify microbial consume rates and is the first to apply ^{13}C-ethane and propane tracers to the water column.

Dissertation Research

The goal of this doctoral work was to calculate the effectiveness of the marine biofilter hypothesis, which states that natural gas released from marine sources, specifically methane, ethane, propane, and butane, is only a minor contribution to the atmospheric reservoir because these gases are readily metabolized by marine microbes. Quantitative tracer methods were developed to track rates of microbial consumption for ethane, propane and butane in a variety of marine environments. These environments included a range of substrate concentrations from low (coastal systems near hydrocarbon reservoirs) to medium (natural seeps) to high (oil spills). The samples containing high substrate concentrations were collected from the Deepwater Horizon oil spill, during and following the nearly three-month hydrocarbon release (Chapter 2). Samples containing low and medium substrate concentrations (Chapters 3, 4) were collected from the world's largest natural marine seep, Coal Oil Point, located offshore of Santa Barbara, California.

References:

Bartlett, K., & R. Harriss (1993), Review and assessment of methane emissions from wetlands. *Chemosphere*, 26(1), 261-320.

Cicerone, R., & R. Oremland (1988). Biogeochemical aspects of atmospheric methane. *Global Biogeochemical Cycles*, 2(4), 299-327.

Coast Guard, United States (2013), Oil Pollution Act Liability Limits in 2013, 1-28.

Etiope, G. & P. Ciccioli (2009). Earth's Degassing: A Missing Ethane and Propane Source. *Science*, 323, 478-478.

Etiope, G., K. Lassey, R. Klusman & E. Boschi (2008). Reappraisal of the fossil methane budget and related emission from geologic sources. *Geophysical Research Letters*, 35, 5.

Fung, I., J. John, J. Lerner, E. Matthews, M. Prather, L. Steele, & P. Fraser (1991). Three-dimensional model synthesis of the global methane cycle. *Journal of Geophysical Research: Atmospheres* (1984–2012), 96(D7), 13033-13065.

Hanson, R., & T. Hanson (1996). Methanotrophic bacteria. *Microbiological reviews*, 60(2), 439-471.

Head, I., D. Jones, & W. Röling (2006). Marine microorganisms make a meal of oil. *Nature Reviews Microbiology*, 4(3), 173-182.

Heintz, M., S. Mau & D. Valentine (2012). Physical control on methanotrophic potential in waters of the Santa Monica Basin, Southern California. *Limnology and oceanography*, 57(2), 420-432.

Kinnaman, F., D. Valentine, & S. Tyler (2007). Carbon and hydrogen isotope fractionation associated with the aerobic microbial oxidation of methane, ethane, propane and butane. *Geochimica Acta*, 71, 271-283.

Kniemeyer, O., F. Musat, S. Sievert, K. Knittel, H. Wilkes, M. Blumenberg, W. Michaelis, A. Classen, C. Bolm, S. Joye & F. Widdel (2007) Anaerobic oxidation of short-chain hydrocarbons by marine sulphate-reducing bacteria. *Nature*, 449, 898-U10.

Levin, S. (2005). Self-organization and the emergence of complexity in ecological systems. *Bioscience*, 55(12), 1075-1079.

Perry, J. J. (1979). Microbial cooxidations involving hydrocarbons. Microbiological Reviews, 43(1), 59.

Plassdulmer, C., R. Koppmann, M. Ratte, J. Rudolph (1995). Light nonmethane hydrocarbons in seawater *Global Biogeochemical Cycles*, 9, pp. 79–100.

Pozzer, A., J. Pollmann, D. Taraborrelli, P. Joeckel, D. Helmig, P. Tans, J. Hueber, & J. Lelieveld (2010). Observed and simulated global distribution and budget of atmospheric C 2-C 5 alkanes. *Atmospheric Chemistry and Physics*, 10(9), 4403-4422.

Redmond, M.C., D.L. Valentine, and A.L. Sessions (2010), Identification of novel methane-, ethane-, and propane-oxidizing bacteria at marine hydrocarbon seeps by stable isotope probing. *Applied and Environmental Microbiology*, 76(19), 6412-6422.

Redmond, M., and D. Valentine (2012), Natural gas and temperature structured a microbial community response to the Deepwater Horizon oil spill, *Proceedings of the National Academy of Sciences*, 109(50), 20292-20297.

Reeburgh, W., B. Ward, S. Whalen, K. Sandbeck, K. Kilpatrickt, & L. Kerkhof (1991). Black Sea methane geochemistry. Deep Sea Research Part A. *Oceanographic Research Papers*, 38, S1189-S1210.

Reeburgh, W.S. (2007), Oceanic methane biogeochemistry, *Chemical Reviews*, 107, 486–513.

Rojo, F. (2009). Degradation of alkanes by bacteria. *Environmental Microbiology*, 11(10), 2477-2490.

Sassen, R., H. Roberts, R. Carney, A. Milkov, D. DeFreitas, B. Lanoil, & C. Zhang (2004). Free hydrocarbon gas, gas hydrate, and authigenic minerals in chemosynthetic communities of the northern Gulf of Mexico continental slope: relation to microbial processes. *Chemical Geology*, *205*(3), 195-217.

Sohngen, N. (1906). Bacteria which use methane as a carbonaceous energy sources. Zentr. Bakt. Parasitenk., Abt II, 15, 513-517.

Valentine D., D. Blanton, W. Reeburgh, M. Kastner (2001). Water column methane oxidation adjacent to an area of active hydratedissociation, Eel River Basin. *Geochim Cosmochim Acta* 65:2633–2640

Valentine, D., J. Kessler, M. Redmond, S. Mendes, M. Heintz, C. Farwell, L. Hu, F. Kinnaman, S. Yvon-Lewis, M. Du, E. Chan, F. Tigreros, C. Villanueva (2010). Propane respiration jump-starts microbial response to a deep oil spill. *Science*, 330(6001), 208-211.

Van Beilen, J., T. Smits, L. Whyte, S. Schorcht, M. Röthlisberger, T. Plaggemeier, K. Engesser, B. Witholt (2002). Alkane hydroxylase homologues in Gram-positive strains. *Environmental microbiology*, 4(11), 676-682.

Figures:

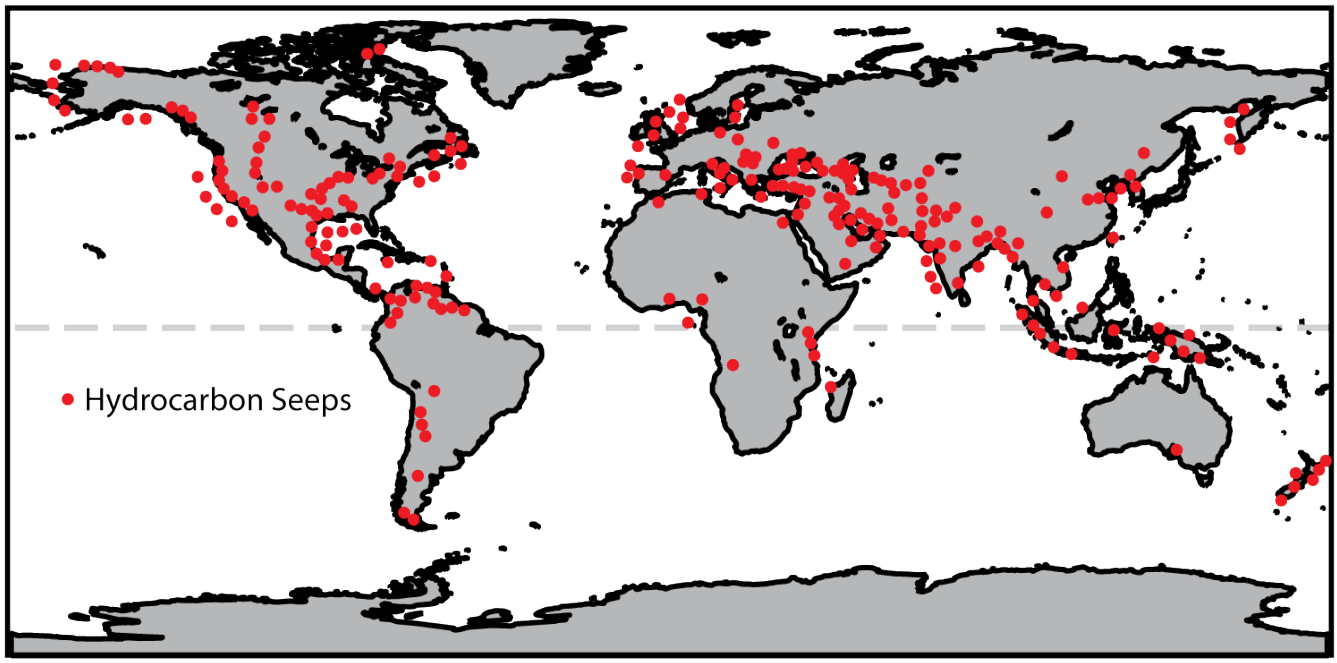

Figure 1. Map showing the global distribution of known hydrocarbon seeps. Modified from Etiope et al. 2009

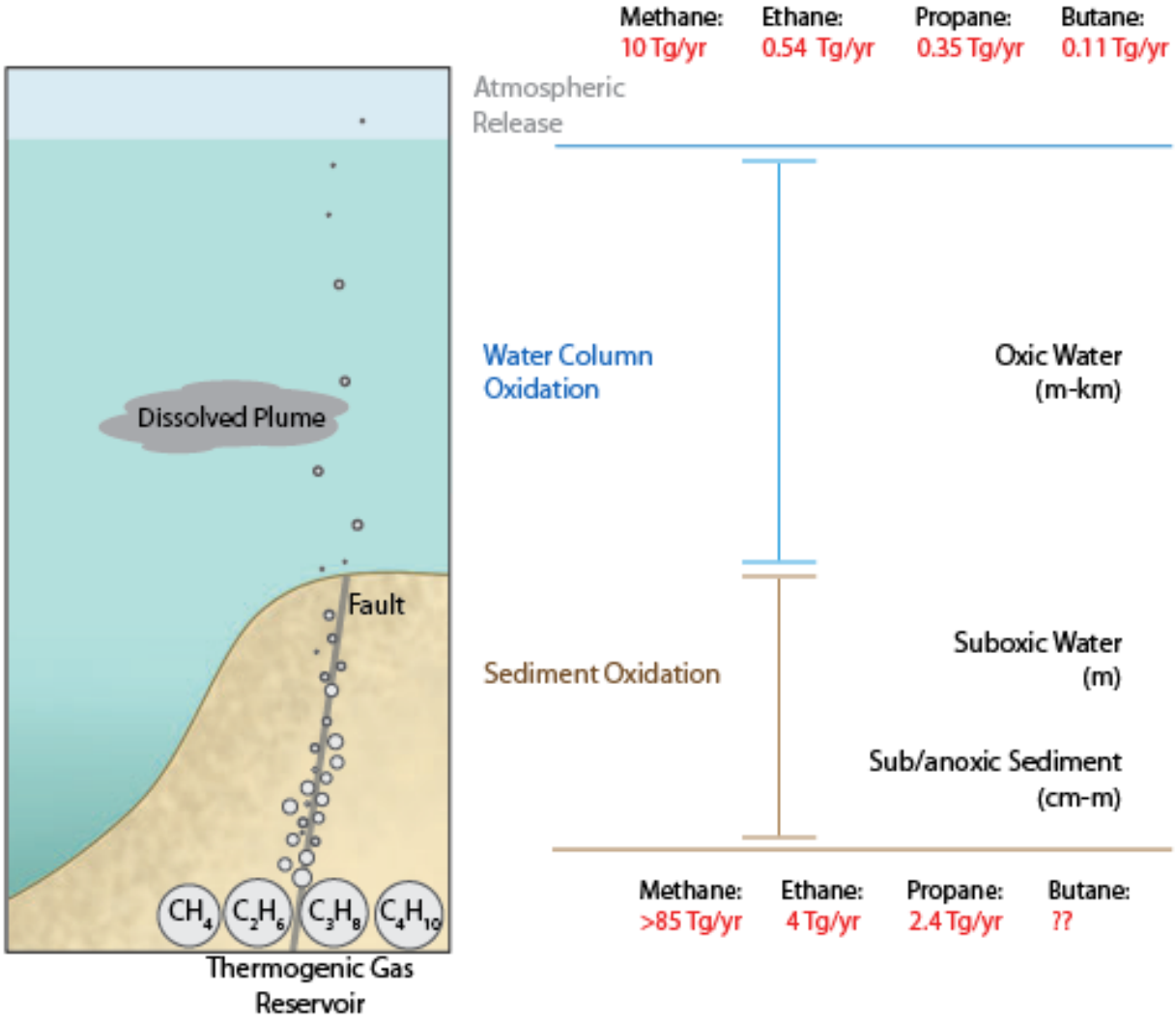

Figure 2. Schematic diagram highlighting hydrocarbon transport and microbial consumption from natural seeps. Reeburgh 2007, Etiope & Ciccioli 2009, Pozzer et al. 2010, Plass-Dulmer et al. 1995.

II. Microbial Consumption of Natural Gas released from the Deepwater Horizon Oil Spill in the Gulf of Mexico

Work presented in this chapter contributed to the following publications:

Valentine, D.L., J.D. Kessler, M.C. Redmond, S.D. Mendes, M.B. Heintz, C. Farwell, L. Hu, F.S. Kinnaman, S. Yvon-Lewis, M. Du, E.W. Chan, F.G. Tigreros, and C.J. Villanueva (2010), Propane Respiration Jump-Starts Microbial Response to a Deep Oil Spill, Science, 330(6001), 208-211. doi:10.1126/science.1196830

Kessler, J.D., D.L. Valentine, M.C. Redmond, M. Du, E.W. Chan, S.D. Mendes, E.W. Quiroz, C. J. Villanueva, S.S. Shusta, L.M. Werra, S.A. Yvon-Lewis, T.C Weber. (2011), A persistent oxygen anomaly reveals the fate of spilled methane in the deep Gulf of Mexico. Science, (6015) 312-315. doi: 10.1126/science.1199697

Abstract

The Deepwater Horizon event was unprecedented because of the quantity discharged and the depth at which the discharge occurred. In response to this event, I sought to assess the importance of ethane and propane oxidation by the indigenous bacterial community. Within 20 weeks of the hydrocarbon release microbial communities had “bloomed" to consume elevated concentrations of ethane and propane, and “busted” following a prolonged period of starvation. This short time interval for complete natural gas consumption contradicts initial predictions and indicates that oxidation rates can accelerate in environments of high substrate concentrations that allow for microbial growth.

1. Introduction

On April 20, 2010, the Deepwater Horizon oil spill released approximately 4.4 million barrels of oil and 1.7×10^{11} g of natural gas into the Gulf of Mexico. The blowout left the well head uncapped for 85 days as the disaster became the largest accidental marine oil spill in the history of the petroleum industry. Natural gas released by the spill consisted predominately of methane, ethane, and propane, at relative abundances of 87.5%, 8.1%, and 4.4%, respectively (Reddy et al., 2012). The event was noteworthy not only because of its scale, but also because it was the first major oil spill to occur at great depth (1500 m), a factor which influenced both the containment effort and the environmental fate of the spilled oil and gas. Rather than bubbling to the surface, natural gas released from the well dissolved into the water column at depths between 1000 and 1200 m. The spill thus provided a rare opportunity to further our understanding of hydrocarbon fate in the ocean.

Hydrocarbons, including oil and gas, are viable substrates for a diversity of microbial communities, each with specific metabolic pathways (Ashraf, 1994; Atlas, 1981; Arp, 1999; Hanson and Hanson, 1996). Methane-consuming bacteria are arguably the most specialized of the hydrocarbon-degrading bacteria as they are limited by their inability to consume multicarbon substrates such as ethane and. Organisms that consume ethane and propane, the other major components of natural gas, remain largely unknown in marine environments, but may include organisms related to methanotrophs or oil-degraders (Redmond and Valentine 2012). It is difficult to predict behavior and response of microbial communities in hydrocarbon-rich settings based on current research. Factors that control methane or natural

gas oxidation remain poorly constrained. Very few direct measurements of marine methane oxidation exist in the literature, and even fewer exist for ethane and propane consumption (Joye et al., 2004; Redmond et al., 2010; Reeburgh, 2007).

This study aimed to resolve the capacity by which microbial communities consume natural gas released from the oil spill. Tracking methane, ethane, and propane oxidation rates in the dissolved plume over its lifespan provides insight into the open ocean's capacity for intrinsic biodegradation.

2. Field Site and Sampling

Samples were collected and treated on board the *R/V Cape Hatteras* between day 53 and 61 (June 12–20, 2010) of the 85 day oil spill and on the National Oceanic and Atmospheric Administration (NOAA) ship *Pisces* about two months following the sealing of the wellhead (September 7-17, 2010) (Figure 1). Due to the chaotic and unprecedented nature of the incident, sampling locations were chosen based on (1) information provided by other vessels tracking the plume, and (2) real-time measurements using a water sampler (CTD rosette) coupled with oxygen, temperature, and fluorescence monitors. The approximate locations of dissolved hydrocarbon plumes were identified by communication with other vessels involved in the spill response operation. The depths of dissolved plumes were located primarily using the oxygen and fluorescence sensors on the CTD rosette. Hydrocarbon plumes exhibited a high fluorescence signal (indicating presence of oil) that typically coincided with a decrease in oxygen (indicating high biological activity) (Figure 2).

3. Methods

3.1 Hydrocarbon Concentration

The concentration of methane, ethane, and propane dissolved in the deep plume after the Deepwater Horizon Oil Spill was measured in June 2010 and again in September. Water samples were collected in 60 mL plastic syringes directly from Niskin bottles attached to the CTD rosette. Each 50 mL water sample was supplemented with a headspace of 10 mL N_2 gas. The samples were shaken vigorously and left undisturbed for ≥12 hours, allowing any dissolved hydrocarbons to equilibrate with the N_2 headspace. Following equilibration, 3 mL samples of headspace gas are injected into a gas chromatograph-flame ionization detector (GC-FID) to determine the concentrations of methane, ethane, and propane (Valentine et al. 2010).

3.2 Rates

Water samples for oxidation rate measurements were collected in 160 mL crimp-top serum bottles directly from Niskin bottles attached to the CTD rosette. To reduce contamination, all sample bottles were overflowed with approximately three volumes of water and immediately capped with butyl rubber stoppers and sealed with aluminum crimp caps. To determine rate measurements, a small volume (5–100 μL) of 99% ^{13}C-labeled methane, ethane, or propane tracer was added to the serum bottles. Samples were then immediately transferred to an incubator or cold room and stored in the dark near *in situ* temperature. Experiments were terminated by injecting the bottles with 0.5 mL of a saturated HgCl solution, effectively halting biological activity. Water samples were also

collected for kill controls and background dissolved inorganic carbon (DIC) measurements. These samples were immediately treated with HgCl to preserve the initial conditions of the water sample. ^{13}C of DIC in seawater was determined using the Finnigan Delta XP isotope ratio mass spectrometer (IRMS) coupled with the Finnigan gas bench. In preparation for sample acidification, 0.5 mL of 85% H_3PO_4 was added to 12 mL septum-sealed vials and purged with ultrapure He. Syringes were used to transfer 1 mL of seawater to each vial. Seawater and acid were mixed and allowed to equilibrate overnight, driving all H_2CO_3, HCO_3^-, and CO_3^{2-} to CO_2. The resulting CO_2 was then sampled by the Finnigan gas bench double needle by introducing He gas into the vial while simultaneously sweeping headspace gas into the instrument. Ten aliquots of the resulting CO_2/He gas mix were delivered to the IRMS via a sample loop and analyzed along with four aliquots of house CO_2 gas, three before and one after the sample aliquots. The IRMS measured the abundance of ions of mass 44 ($^{12}CO_2$), 45 ($^{13}CO_2$), and 46 ($^{14}CO_2$), permitting calculation of 45:44 and 46:44 ratios. ^{13}C values were calculated with reference to the laboratory house CO_2 gas. The data were then normalized using LSVEC Li_2CO_3 isotope reference material. The LSVEC was dissolved in low total organic carbon deionized water and treated exactly as the seawater samples. Reproducibility of the ^{13}C analysis was determined by replicate analyses of both LSVEC and a 0.3% CO_2-in-He house check standard. The 0.3% CO_2 check standard also provided for comparison between analytical runs.

3.3 Rate Calculations

Aerobic oxidation of methane, ethane, and propane follow the reactions below (EQ 1-3) (Ashraf et al. 1994, Redmond et al. 2010):

(EQ 1) Methane:

$$^{13}CH_4 + O_2 \rightarrow H_2O + {}^{13}CO_2 + \{Biomass\}$$

(EQ 2) Ethane:

$$^{13}C_2H_6 + O_2 \rightarrow H_2O + {}^{13}CO_2 + \{Biomass\}$$

(EQ 3) Propane:

$$^{13}C_3H_8 + O_2 \rightarrow H_2O + {}^{13}CO_2 + \{Biomass\}$$

*Not balanced reactions (to account for biomass)

Fractional turnover rate (k') represents the consumption capacity of a microbial community under first order kinetic conditions and is calculated by measuring the product of respiration, $^{13}C\text{-}CO_2$, after incubation with the ^{13}C tracer (EQ 4). Fractional turnover rate is only dependent on three variables, (1) normalized moles of CO_2, (2) incubation time, and (3) moles of tracer; however, normalized CO_2 includes factors such as experimental conditions and known isotopic constants (EQ 5). Calculating the normalized moles of CO_2 is demonstrated in Equation 5 using the isotopic values obtained from the IRMS and known isotopic constants.

(EQ 4) $$k' = \frac{\text{Normalized moles of } CO_2}{(\text{Incubation time})\cdot(\text{moles of tracer})}$$

(EQ 5)

$$\text{Normalized moles of } CO_2 = \frac{\left(Background\ moles\ of\ CO_2 * \left(\left(\left(\frac{\delta^{13}C_{Rate\ Sample}}{1000}\right)+1\right)*0.0112372\right) - \left(\left(\left(\frac{\delta^{13}C_{Background}}{1000}\right)+1\right)*0.0112372\right)\right)}{Number\ of\ Carbons\ in\ Tracer}$$

4. Results and Discussion

4.1 Hydrocarbon concentration within the plume

Dissolved hydrocarbon concentrations within background samples of up to 65 nM for methane are common in coastal waters of the Gulf of Mexico. Many natural marine seeps release a consistent supply of gas into the overlying water column here (Kennicutt et al., 1985). Plume samples collected in June, within the period of active petroleum discharge from the ruptured wellhead, reached 126 µM for methane, 10 µM for ethane, and 5 µM for propane, about seven orders of magnitude higher than background (Table 1). By September, dissolved hydrocarbon concentrations for all three gases in plume samples were back to pre-spill levels.

Relative gas ratios varied within plume locations. The methane/ethane and methane/propane ratios help to determine the relative ages of plume samples. Methane/ethane and methane/propane ratios were initially 10.85 and 19.8, respectively, but only increased with time (Figure 3 and Table 1). This shift toward methane (i.e., preferential removal of ethane and propane) is a result of microbial oxidation preferences (Kinnaman et al., 2007; Mau et al., 2007; Valentine et al., 2010). Methanotrophic consumption generally occurs more slowly than microbial consumption of its longer chain analogs, gradually shifting the relative ratios of these gases to favor methane. As the plume aged and sustained methanotrophic oxidation, nearly the entirety of methane was removed by September.

4.2 Microbial Consumption Rate Measurements

The microbial capacity for methane, ethane, and propane biodegradation was measured in freshly collected samples. Only the June data recorded elevated microbial activity (Figures 4 and 5). Time series measurements from June reveal an initial stage where the ^{13}C-CO_2 product accumulates at a constant rate, followed by a marked increase after 24 hours (Figure 7). During the first 24 hours of incubation, production of CO_2 is linear for ethane and propane with R^2 values of 0.92 and 0.94, respectively (Figure 7). The initial rate is interpreted as the maximum potential rate of biodegradation by the basal population, with saturation of the population's enzymatic capacity leading to zeroth-order kinetic behavior. The later increase then indicates a growth, or biosynthetic response, by the microbial community to the elevated substrate level. The concentration series measurements show consumption rates reached a maximum when ≥50 μL tracer is used; implying that these bacteria are not reaching their maximum potential oxidation rates at ambient substrate levels. Therefore any measurements made within 24 hrs of excess substrate injections yield rate measurements under zeroth-order kinetic behavior where consumption rate measurements represent the maximum capacity for hydrocarbon consumption in the deep plume.

4.3 Plume Evolution

Microbial gene-sequence data collected in June 2010 (Kessler et al. 2011, Redmond and Valentine 2012) showed a substantial population of ethane- and propane-consuming

bacteria in the water column, consistent with the high oxidation rates reported in Figures 4 and 5. Ethane- and propane-consuming bacteria during the June expedition were blooming and actively depleting the water of these gases at an average fractional turnover rate of 0.0275 day^{-1} and 0.0502 day^{-1}, respectively, which corresponds to a residence time of 40 days for ethane, and 20 days for propane. Samples collected roughly three months later, in September 2010, had plume waters with (1) near-zero concentrations of ethane and propane and (2) a fractional turnover rate of 0.00831 day^{-1} for ethane and a rate indistinguishable from background for propane. Depletion of natural gas by September is attributed to the blooming microbial communities reported in June. Following complete substrate removal, microbial oxidation rates also fell to background or near background levels by September.

Excess methane was also absent from the deep plume in September; however, the measured methane oxidation rates do not reflect active consumption in either June (0.0011 day^{-1}) or September (0.0013 day^{-1}) regardless of tracer volume and incubation time. The absence of methane from the September deep plume samples is likely due to a bloom of methane oxidizers after the June expedition that depleted the waters of methane before September. Microbial data collected from the September expedition (Kessler et al. 2011) also show an increase in methanotrophs in the bacterial community, which were not detected in most June samples. Although September methane consumption rates were low, the presence of methanotrophs and the absence of methane imply that these waters had previously contained elevated levels of methane.

After complete consumption of dissolved methane, methanotrophs are expected to adapt to the new substrate-depleted conditions and stop active metabolism. Marine bacteria

typically have a mechanism to survive prolonged periods without an external energy source, allowing bacterial cells to persist until conditions become favorable (Amy et al., 1983). However, this starvation regime cannot persist indefinitely. Laboratory studies by Roslev et al. (1994) showed that the methane oxidation ability of substrate-starved methanotrophs decreased exponentially with the length of the starvation period. After 42 days, methane-starved cultures showed no detectable oxidation activity. Thus, the three weeks that elapsed between modeled hydrocarbon drawdown and September sampling could account for the low methane oxidation rates: even though the population of methanotrophs present in the deep plume is large, it is unlikely that the microbes had remained active in the weeks preceding the September expedition. Predation on the methanotrophic community leading to remineralization is also expected to have contributed loss of activity in the aged plume waters.

5.0 Conclusion

Naturally occurring marine microorganisms played a significant role in reducing the overall environmental impact of the Deepwater Horizon oil spill. Results presented herein suggest that natural gas-consuming microbes responded and adapted to the large input of substrate into the ocean caused by the spill. Within 20 weeks of the hydrocarbon release, microbial communities had already “bloomed" at high concentrations of natural gas and “busted” following a prolonged period of starvation. The aging plume’s preferential oxidation of ethane and propane, which was occurring at a high rate in June, shifted gas ratios towards a greater proportion of methane. By September, gas concentrations were

below background in these plumes, including methane. The short time interval for complete natural gas consumption contradicts initial predictions of prolonged exposure and indicates that oxidation rates accelerate in the deep ocean given high substrate concentrations that allow for microbial growth.

Figures:

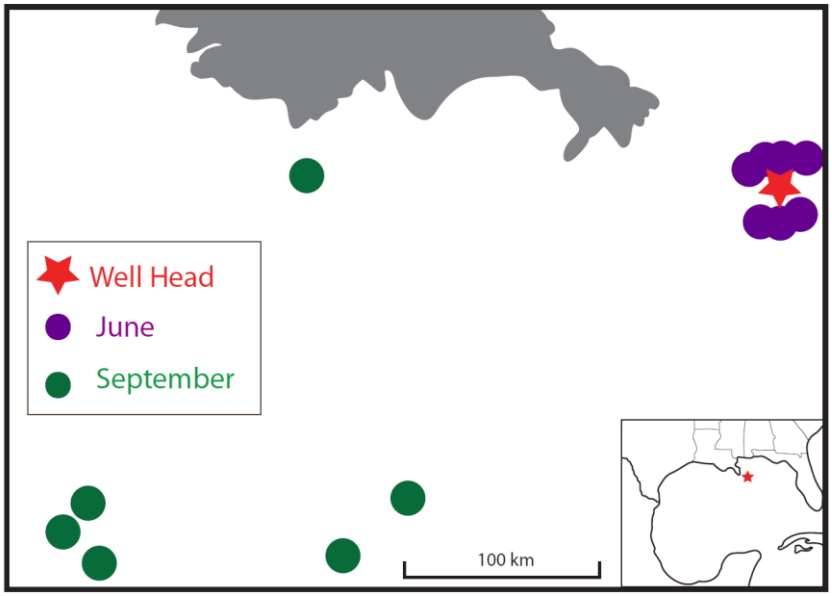

Figure 1. Map of the sampling locations in the Gulf of Mexico.

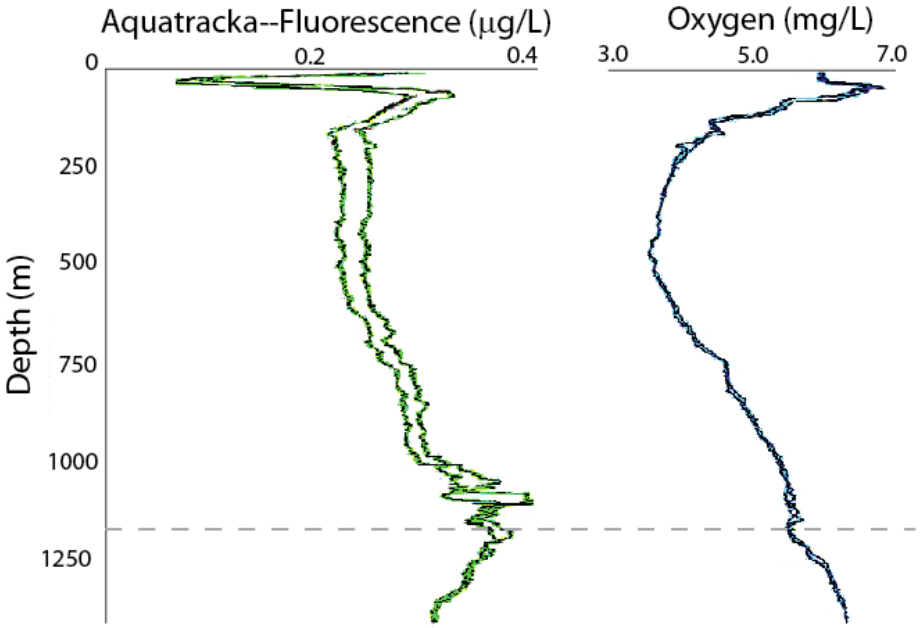

Figure 2. Depth profile collected in September showing the plume depth at 1065 m (dashed line), where a fluorescence peak coincides with an oxygen sag.

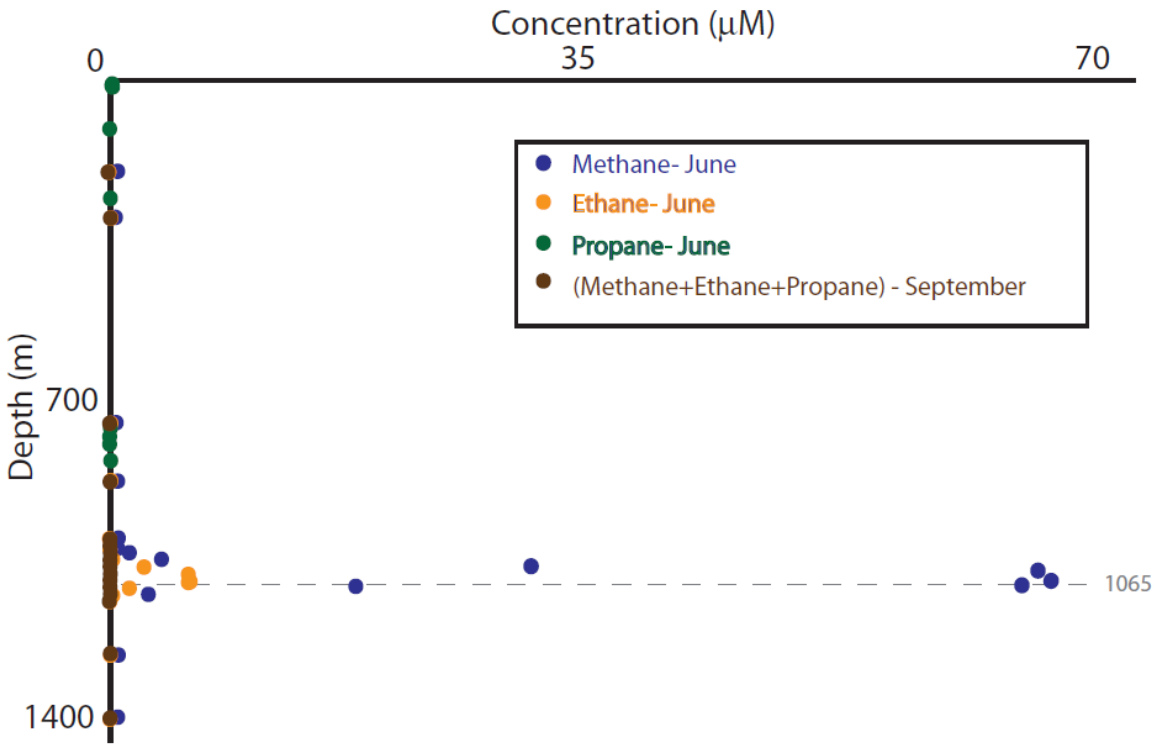

Figure 3. Depth profile for hydrocarbon gas concentrations for June and September.

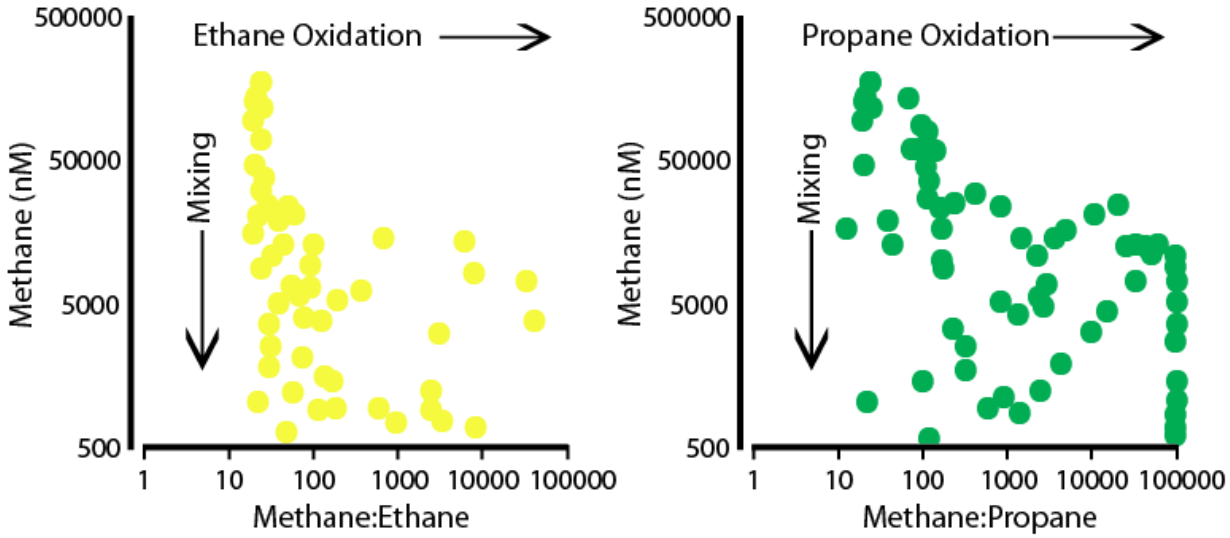

Figure 4. Left panel: Methane:Ethane ratio, Right panel: Methane:Propane

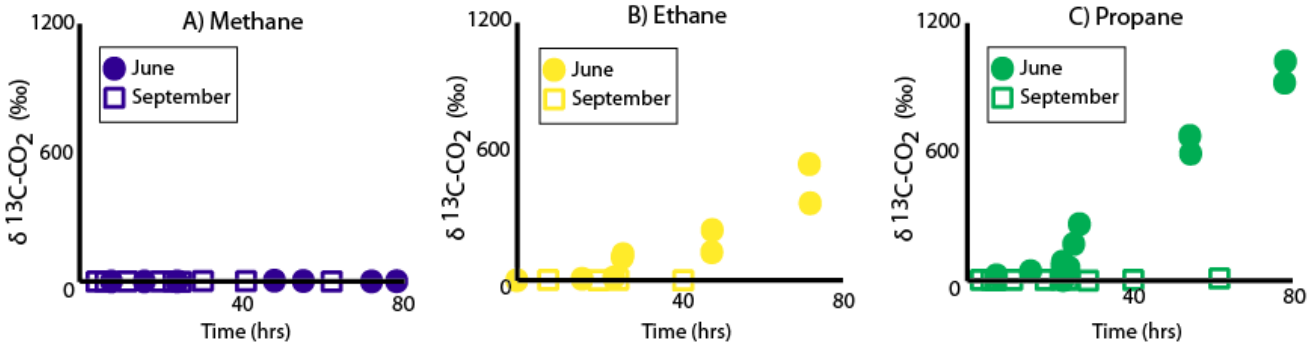

Figure 5. Time Series: For each sample, 100 mL of 99.9% ^{13}C-tracer was used

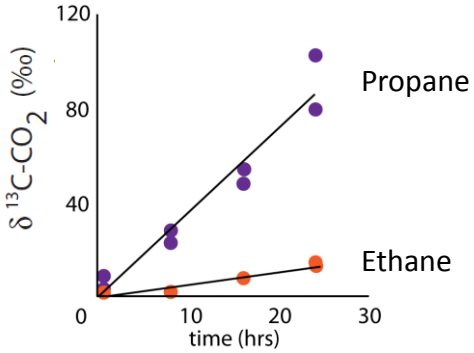

Figure 6. Zoom-in if the first 24 hours of incubation from figure 5. Production of CO_2 is linear for ethane and propane with R^2 values of 0.92 and 0.94, respectively.

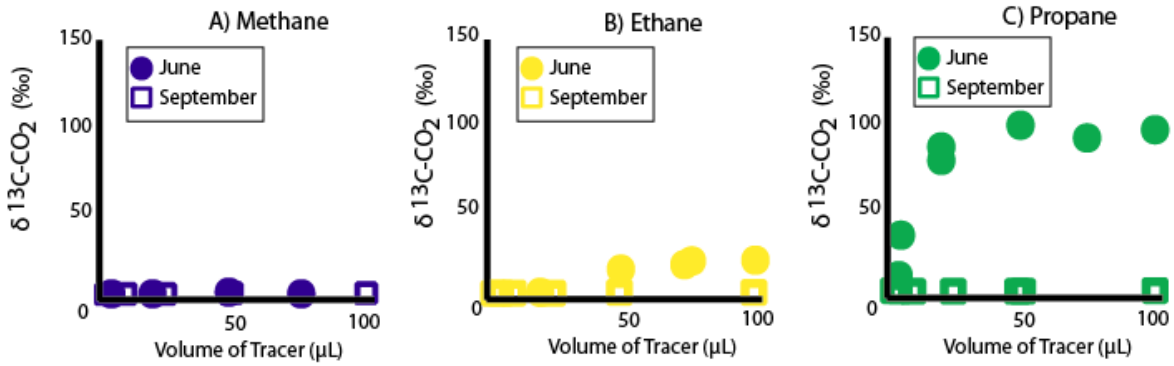

Figure 7. Concentration Series: for each sample, 99.9% ^{13}C-tracer gas was used and incubated for 24 hours.

Table 1. Select properties of samples from June of the dissolved hydrocarbon plume.

Stations	**Latitude** 28°N	**Longitude** 88°W	**Plume Depth** (m)	**[CH_4]** (nM)	**[C_2H_6]** (nM)	**[C_3H_8]** (nM)
07	43.911'	22.606'	910	4600	110	BD*
08	42.244'	25.261'	1026	2800	5	BD*
10	44.975'	22.003'	882	4200	134	3
15	48.435'	26.898'	1120	48000	4100	440
18	40.370'	18.668'	883	3500	BD*	BD*
20	42.204'	16.768'	839	7200	200	BD*
21	43.311'	16.328'	810	6400	290	3
22	44.487'	16.328'	801	13000	940	300
23	45.531'	16.328'	848	11000	600	5
24	46.750'	16.328'	898	29000	1800	70
25	47.550'	17.328'	875	14000	630	10

*BD represents samples that were below analytical detection limit.

References:

Amy, P. S., & Morita, R. Y. (1983). Starvation-survival patterns of sixteen freshly isolated open-ocean bacteria. *Applied and environmental microbiology*, 45(3), 1109-1115.

Arp, D. J. (1999), Butane metabolism by butane-grown 'Pseudomonas butanovora', *Microbiology*, 145(5), 1173-1180.

Ashraf, W., A. Mihdhir, and C.J. Murrell (1994), Bacterial oxidation of propane. *FEMS Microbiology Letters*, 122(1), 1-6.

Atlas, R. M. (1981). Microbial degradation of petroleum hydrocarbons: an environmental perspective. *Microbiological reviews*, 45(1), 180.

Hanson, R. S., & Hanson, T. E. (1996). Methanotrophic bacteria. *Microbiological reviews*, *60*(2), 439-471.

Joye, S. B., Boetius, A., Orcutt, B. N., Montoya, J. P., Schulz, H. N., Erickson, M. J., & Lugo, S. K. (2004). The anaerobic oxidation of methane and sulfate reduction in sediments from Gulf of Mexico cold seeps. *Chemical Geology*, 205(3), 219-238.

Kennicutt, M. C., Brooks, J. M., Bidigare, R. R., Fay, R. R., Wade, T. L., & McDonald, T. J. (1985). Vent-type taxa in a hydrocarbon seep region on the Louisiana slope. *Nature*, 317(6035), 351-353.

Kessler, J.D., D.L. Valentine, M.C. Redmond, M. Du, E.W. Chan, S.D. Mendes, E.W. Quiroz, C. J. Villanueva, S.S. Shusta, L.M. Werra, S.A. Yvon-Lewis, T.C Weber. (2011), A persistent oxygen anomaly reveals the fate of spilled methane in the deep Gulf of Mexico. Science, (6015) 312-315. doi: 10.1126/science.1199697

Kinnaman, F.S., D.L. Valentine, and S.C. Tyler (2007), Carbon and hydrogen isotope fractionation associated with the aerobic microbial oxidation of methane, ethane, propane and butane, *Geochim. Cosmochim. Acta*, 71, 271–283.

Mau S, Valentine DL, Clark JF, Reed J, Camilli R, Washburn L (2007). Dissolved methane distributions and air-sea flux in the plume of a massive seep field, Coal Oil Point, California. *Geophys. Res. Lett.* 34:L22603. doi:10.1029/2007GL031344

Redmond, M.C., D.L. Valentine, and A.L. Sessions (2010), Identification of novel methane-, ethane-, and propane-oxidizing bacteria at marine hydrocarbon seeps by stable isotope probing. Applied and Environmental Microbiology, 76(19), 6412-6422.

Redmond, M.C., and D.L. Valentine (2012), Natural gas and temperature structured a microbial community response to the Deepwater Horizon oil spill, *Proceedings of the National Academy of Sciences*, 109(50), 20292-20297. doi:10.1073/pnas.1108756108

Roslev, P., & King, G. M. (1994). Survival and recovery of methanotrophic bacteria starved under oxic and anoxic conditions. *Applied and environmental microbiology*, 60(7), 2602-2608.

Valentine, D.L., J.D. Kessler, M.C. Redmond, S.D. Mendes, M.B. Heintz, C. Farwell, L. Hu, F.S. Kinnaman, S. Yvon-Lewis, M. Du, E.W. Chan, F.G. Tigreros, and C.J. Villanueva (2010), Propane Respiration Jump-Starts Microbial Response to a Deep Oil Spill, *Science*, 330(6001), 208-211. doi:10.1126/science.11968

III. Marine Microbes Rapidly Adapt to Consume Ethane, Propane, and Butane within the Dissolved Hydrocarbon Plume of a Natural Seep

Work presented in this chapter has been submitted to JGR: Oceans

Complete list of authors: Molly C. Redmond, Karl Voigritter, Christian Perez, Rachel Scarlett, and David L. Valentine

Abstract

Simple hydrocarbon gases containing two to four carbons (ethane, propane, and butane) are among the most abundant compounds present in petroleum reservoirs, and are introduced into the ocean through natural seepage and industrial discharge. Yet little is known about the bacterial consumption of these compounds in ocean waters. To assess the timing by which microbes metabolize these gases, a 3-phase study tested and applied a radiotracer-based method to quantify the oxidation rates of ethane, propane and butane in fresh seawater samples. Phase 1 involved the synthesis of tritiated ethane, propane, and butane using Grignard reagents and tritiated water. Phase 2 was a systematic assessment of experimental conditions, wherein the indigenous microbial community was found to rapidly oxidize ethane, propane, and butane. Phase 3 was the application of this tritium method near the Coal Oil Point seeps, offshore California. Spatial and temporal patterns of ethane, propane, and butane oxidation down current from the hydrocarbon seeps demonstrated that >99% of these gases are metabolized within 1.3 days following initial exposure. The oxidation of ethane outpaced oxidation of propane and butane with a pattern suggesting the

microbial community responded to these gases by rapid adaptation or growth. Methane oxidation responded the slowest in plume waters. Estimates based on the observed metabolic rates and carbon mass balance suggest that ethane, propane, and butane consuming microorganisms may transiently account for a majority of the total microbial community in these impacted waters.

1. Introduction

Thermogenic hydrocarbon gases generated in the deep subsurface are among the most abundant compounds in petroleum deposits. For example, ethane, propane, and butane together accounted for ~9% of the mass discharged from the Macondo well during the Deepwater Horizon event, the most abundant individual compounds after methane [*Reddy et al.,* 2012]. The emission of hydrocarbon gases into the ocean and atmosphere can have significant environmental repercussions. Understanding the interplay between physical and microbiological controls is the motivation for this research.

Ethane, propane, and butane biogeochemistry is relatively unstudied compared to methane, which serves as an important benchmark for comparison. Methane is the most abundant of these gaseous hydrocarbons and the most potent as a greenhouse gas [*Cicerone and Oremland,* 1988; *Etiope et al.,* 2008; *Fung et al.,* 1991]. Current estimates suggest that 75-310 Tg of methane is released into the ocean each year, but only ~10 Tg of that methane reaches the atmosphere [*Reeburgh,* 2007]. The majority of methane is consumed by marine microorganisms, which act as an effective biofilter [*Reeburgh, 2007*].

Ethane, propane, and butane are also greenhouse gases [*Collins et al.,* 2002] and precursors to atmospheric pollutants such as acetone, alkyl nitrates, and ozone [*Jacob et al.,* 2002; *Katzenstein et al.,* 2003; *Singh et al.,* 1994]. Their emissions into the ocean are estimated as 0.54, 0.35, and 0.11 Tg/yr, respectively [*Plass-Dulmer et al.,* 1995]. However, natural seep environments were not considered in these estimates and may provide an important contribution. For example, the Coal Oil Point seep field in the Santa Barbara Channel releases 4.9×10^9 g/yr of ethane and propane, equivalent to ~1% of ocean emissions, with only half of this discharge reaching the atmosphere as bubbles rising to the sea surface [*Clark et al*., 2000]. The remainder of the gas dissolves into the water column and is transported away from the seep by ocean currents [*Mau et al*., 2010; 2007]. The partitioning of the dissolved gas between atmospheric flux and biological consumption remains uncertain.

The biogeochemical importance of these gases has been highlighted by a series of recent industrial incidents. In 2010, the Deepwater Horizon well blowout in the Gulf of Mexico caused the world's largest accidental marine oil discharge. In addition to oil, an estimated 1.7×10^{11} g of natural gas was released into the ocean over 85 days [*Reddy et al.,* 2012]. The event was noteworthy not only because of its scale, but also because the oil and gas were discharged to the ocean at a depth of 1500 meters. At this depth, virtually all the ethane, propane, and butane dissolved into the water column. Ethane and propane (and probably butane) were consumed by bacteria within weeks after discharge [*Valentine et al.,* 2010], with propane alone accounting for up to ~60% of total respiration in some samples.

While the importance of ethane, propane, and butane during subsea discharge events is now recognized, there is still minimal understanding as to the factors responsible for a microbial response. Even after the Deepwater Horizon event, the continued occurrence of petroleum spills [*Coast Guard,* 2013] and gas blowouts in particular (e.g., Elgin field blowout in the North Sea and the Hercules 265 blowout in the Gulf of Mexico) demonstrate that such events happen frequently enough to argue for an improved understanding of the oceanographic effects of ethane, propane, and butane discharge.

Microbial oxidation is a major control on the atmospheric release of oceanic methane, ethane, propane, and butane. Marine bacteria are known to oxidize these gases and are presumed to do so by first converting the hydrocarbon to its analogous alcohol and water, followed by conversion to carbon dioxide, biomass and additional water [*Arp,* 1999; *Ashraf et al.,* 1994; *Hanson and Hanson,* 1996; *Perry,* 1980], as shown in equations 1-4. Previous studies have focused on the biochemistry of methane oxidation and the ecology of responsible bacteria [*Hanson and Hanson,* 1996; *Reeburgh,* 2007; *Valentine,* 2011]. Comparatively few studies have considered ethane, propane, and butane consumption, particularly in the marine realm. For example, the anaerobic oxidation of methane (AOM) has been studied since the late 1960s [*Reeburgh,* 1969], whereas the anaerobic oxidation of ethane, propane, and butane has only recently been investigated [*Adams et al*., 2013; *Mastalerz et al*., 2009; *Kniemeyer et al*., 2007; *Quistad et al*., 2011].

(EQ 1) Methane:

$$CH_4 + 2O_2 \rightarrow \{CH_3OH\} \rightarrow CO_2 + 2H_2O + \{\text{Biomass}\}$$

(EQ 2) Ethane:

$$C_2H_6 + 3.5O_2 \rightarrow \{C_2H_5OH\} \rightarrow 2CO_2 + 3H_2O + \{Biomass\}$$

(EQ 3) Propane:

$$C_3H_8 + 5O_2 \rightarrow \{C_3H_7OH\} \rightarrow 3CO_2 + 4H_2O + \{Biomass\}$$

(EQ 4) Butane:

$$C_4H_{10} + 6.5O_2 \rightarrow \{C_4H_9OH\} \rightarrow 4CO_2 + 5H_2O + \{Biomass\}$$

One critical factor for predicting the impact of ethane, propane, and butane input to the ocean is understanding the response of the microbial community. This specifically pertains to the timeframe for adaptation of the microbial community to respire these gases. ^{13}C-labeled tracers were used to measure propane oxidation rates in anoxic sediments of a hydrocarbon seep as well as ethane and propane oxidation rates after the Deepwater Horizon oil spill [*Quistad and Valentine*, 2011; *Valentine et al.*, 2010]. However, the ^{13}C-tracer method is relatively insensitive and its utility is limited to environments where the ambient gas concentrations are high and the conversion of ^{13}C is detectable above background levels of dissolved inorganic carbon. In most environments, a more sensitive tracer is required to effectively quantify oxidation rates.

Herein, we developed and applied a tritium-based tracer method for quantifying respiration rates for ethane, propane, and butane. Our methods were modeled after the

tritiated-methane method of *Reeburgh et al.*, [1991] as modified by *Valentine et al.* [2001]. This study reports new experimental techniques and applications to natural samples with the goal of tracking microbial oxidation of ethane, propane, and butane dissolved into the ocean. These experiments are described in three phases: Phase 1, synthesis of tritiated hydrocarbon tracers; Phase 2, tests of the tracer's efficacy for quantifying hydrocarbon respiration rate in fresh seawater samples; Phase 3, tritium tracer application for tracking spatial and temporal patterns of hydrocarbon oxidation after exposure at a natural hydrocarbon seep.

2. Method

2.1 Method Development and Assessment (Phase 1)

2.1.1 Synthesis

Tritiated tracers were synthesized using Gringard reagents and tritiated water. All reactions were performed using oven-dried glassware under an atmosphere of dry helium. The Grignard reagents ethylmagnesium bromide, propylmagnesium chloride, and butylmagnesium bromide are commercially available from Sigma Aldrich and were used as received (2M in tetrahydrofuran). Tritiated water (a mixture of H_2O and HTO) was purchased from Moravek Biochemicals (20.83 Ci/mL in dry tetrahydrofuran.) All reactions were performed in 5 mL serum bottles sealed with butyl rubber stoppers. The resulting gases were transferred to 12 mL serum bottles using 1/16" stainless steel tubing attached to two valves (Figure 1). Concentrations were measured using a gas chromatograph coupled to a flame ionization detector and activity was determined with a Beckman LS6500 liquid scintillation counter, with associated errors of 6 nM and 0.2 μCi, respectively.

2.1.1.1Representative Tritium Labeling Procedure; ethane-1-t

The general experimental procedure was adapted from a deuterium labeling synthesis outlined in *Olszowy* [1984] (Equations 5-8).

An ethylmagnesium bromide solution (100 μL, 0.2 mmol) was added to an oven dried, He purged 5 mL serum bottle sealed with a butyl rubber stopper via a dried syringe. The solution was cooled to 0 °C, and the tritiated water solution (68 μL, 0.08 mmol) was added dropwise. The reaction was allowed to warm to room temperature and was stirred overnight. The tritiated gas was then transferred to an evacuated bottle for storage. This was carried out using a dry custom-made Swagelok transfer line consisting of 1/16" OD stainless steel tubing equipped with two-way stainless steel valves on each end (Figure 1). The gas was passed through a "solvent trap" which consisted of a portion of the transfer line being immersed in a dry ice/acetone cooling bath to trap any residual THF.

(EQ 5) General: $R\text{-}MgX + HTO \rightarrow R\text{-}H \text{ or } R\text{-}H$

(EQ 6) Ethane: $C_2H_5\text{-}MgBr + HTO \rightarrow C_2H_5T \text{ or } C_2H_6$

(EQ 7) Propane: $C_3H_7\text{-}MgCl + HTO \rightarrow C_3H_7T \text{ or } C_3H_8$

(EQ 8) Butane: $n\text{-}C_4H_9\text{-}MgBr + HTO \rightarrow C_4H_9T \text{ or } C_4H_{10}$

2.2 Method Assessment (Phase 2)

2.2.1 Method Assessment Study Site

Samples were collected from the *R/V Atlantis* in September 2011. Water for the method assessment study was collected during one cast of a 24-bottle Niskin rosette at station Plume 3 (Table 1, Figure 2), 10.5 km down-current from Coal Oil Point. For reference, Coal Oil Point emits > 10^{10} g/yr of natural gas with a composition of 87.5% methane, 5.1% ethane, and 3.1% propane, along with trace amounts of heavier hydrocarbons [*Clark et al*., 2000; *Mau et al*., 2010]. Though these seeps are relatively shallow (ranging from 5-80 meters) [*Hornafius and Quigley*, 1999], *Clark et al*. [2000] calculated that 3.6 x 10^6 mol d^{-1}, 2.1 x 10^5 mol d^{-1}, 1.2 x 10^5 mol d^{-1}, and 3.7 x 10^4 mol d^{-1} of methane, ethane, propane, and butane, respectively, are dissolved into the water. Of that, only 1% of methane and less than 1% of ethane and propane is transferred to the atmosphere in the immediate vicinity of the seeps [*Mau et al*., 2010; 2013].

2.2.2 Tritium Tracer Method

The method for ethane, propane, and butane oxidation rate measurements was adapted from previously published procedures for methane [*Reeburgh et al*., 1991; *Valentine et al*., 2001]. The five general steps are as follows: (1) collect seawater samples in 160 mL serum bottles, seal with a chlorobutyl stopper and metal crimp cap, take replicates for ambient concentration measurement, (2) add tritiated gas to samples via gas-tight syringe and incubate, (3) add mercuric chloride (0.5 mL of a saturated water solution) to halt further consumption of the tracer and sparge with a nonradioactive gas, such as air, to remove any unreacted tracer (4) measure activity in the sample (amount of tracer consumed) using a

liquid scintillation counter (LSC), (5) calculate rate of microbial consumption using equations 9-13. For kill controls, Step (3) is done prior to Step (2).

Methane oxidation rates were also measured during the method assessment as a comparison, using the same five steps outlined. Samples were injected with 10 μCi of methane tracer (100 μl of 0.1 Ci/L tritiated methane stock) and incubated for 24 hours near *in situ* temperature.

2.2.3 Ambient Hydrocarbon Concentration Analysis

Ambient concentrations of dissolved methane, ethane, propane, and butane were determined using established techniques [*Heintz et al*., 2012; *Mau et al.*, 2010; *Valentine et al*., 2001]. Seawater samples were transferred to 160 mL serum bottles, and dissolved gas from the sample bottle was exsolved by replacing 10 mL of seawater with 10 mL of ultrapure N_2 gas. To inhibit microbial activity, mercuric chloride was added to all samples intended for concentration analysis. Samples were shaken vigorously and allowed to equilibrate for a minimum of 12 hours. Headspace concentrations were measured with a gas chromatograph coupled to a flame ionization detector (GC-FID; Shimadzu Corp. 14A) and run isothermally (60 °C) using N_2 as the carrier gas through a 12' x 1/8"packed column (n-octane on Res- Sil C). Analytical error from GC-FID measurements, based on previous application of this method, was ±5%.

2.2.4 Calculating Oxidation Rates

The fraction of hydrocarbon tracer converted to aqueous-phase product (f_{ox}) is calculated directly from the ratio of tracer consumed (activity of tritium in the aqueous phase, A_{aq}) to amount of tracer injected (total activity of tritium tracer injected, A_i), after accounting for abiotic contributions as quantified by kill controls (activity of tritium from abiotic sources, A_x).

(EQ 9) $f_{ox} = (A_{aq} - A_x)/(A_i - A_x)$

Because A_x is typically very small compared A_i, f_{ox} can be simplified as:

(EQ 10) $f_{ox} = (A_{aq} - A_x)/(A_i)$

By accounting for the incubation time (t_i) the fractional turnover rate of tritium-labeled tracer (k'), can be calculated as:

(EQ 11) $k' = f_{ox}/t_i$

Assuming the tracer behaves identically to the unlabeled substrate (i.e., complete mixing and no isotope effects), the average rate of substrate consumption in the sample (R_b) can be calculated from the molar concentrations of labeled substrate (concentration of tritium-labeled substrate added to the sample, S_T) and the initial substrate (concentration of substrate present in the sample at the time the tracer was injected, S_e):

(EQ 12) $R_b = k' * [S_T + S_e]$

For the sake of clarity, this study reports primarily the fractional turnover rate (k') as a metric of substrate consumption.

Under select conditions these equations can be expanded to calculate the oxidation rate of substrate in-situ (i.e., the rate at which substrate in the sample would be consumed if not removed from its natural environment, R_e), as is typically done for the calculation of methane oxidation rate [*Valentine et al.*, 2001]. Necessary conditions include: (1) oxidation rate is linearly dependent on the substrate concentration (first order kinetic behavior), (2) the microbial community is neither in growth nor decline with respect to the substrate being studied, (3) the microbial community is not primed by the addition of exogenous substrate, and (4) the conditions of sampling and incubation do not affect the capacity of the microbial community to consume substrate. Thus the rate of substrate consumption may be expressed in a first order form:

(EQ 13) $R_e = k' * [S_e]$

Note that results of this study deviate from the form of EQ 13, and the significance of these deviations are considered in Section 4.1. Replicate samples measured on the LSC had an average error of ± 0.2 nCi.

2.2.5 Comparison with Established ^{13}C Method

To compare sensitivity between ^{3}H- and ^{13}C-tracer methods, oxidation rate experiments using both tracers were run in parallel for ethane and propane. Rate

measurements with ^{13}C were performed using a similar approach to those reported by *Valentine et al*., [2010]. A small volume (5–100 μL) of 99% ^{13}C-labeled ethane or propane tracer was injected into each sample. Water samples were also collected for kill controls and background dissolved inorganic carbon (DIC) measurements. The ^{13}C of DIC in seawater was determined using the Finnigan Delta XP Isotope Ratio Mass Spectrometer (IRMS) coupled with the Finnigan Gas Bench. Oxidation rates are calculated using the same rate equation as the tritium approach (EQ 13); however, the fractional turnover rate is calculated using equations 14 and 15.

(EQ 14) k = (normalized moles of CO_2) / ((incubation time) * (moles of tracer))

(EQ 15) Normalized moles of CO_2 =

(Background moles of CO_2 * (((δ ^{13}C $_{rate\ sample}$ /1000) +1) *0.0112372) – (((δ ^{13}C $_{background}$/1000) +1) *0.0112372)) / number of carbons in tracer

2.3 Method Application – Oxidation within a Plume (Phase 3)

2.3.1 Sample Collection

Seawater samples were collected in California's Santa Barbara Channel (Figure 2, Table 2) from aboard the *R/V Atlantis* (September 2011) and the *M/V Connell* (June-September 2012). Identifying and tracking the dissolved plume was the greatest challenge associated with sample collection. Since the samples were collected while the currents were flowing westward, north-south transects were conducted in an attempt to intersect the core

of the plume. The plume's core was identified by collecting water at depths from 35-55 m at each station along the N-S transect, and analyzing the samples for hydrocarbon content shipboard using a GC-FID. Seawater samples for subsequent analysis were collected only at the station and depth where the maximum hydrocarbon signal was observed for each N-S transect. The N-S transects were spaced ~1.5 km apart and samples from the plume's core were analyzed for dissolved hydrocarbon concentration and ethane, propane, and butane oxidation rates.

2.3.2 Oxidation Rates in the Plume

Oxidation rates were determined using the five steps described in Section 2.2.2 (Tritium Tracer Method). The experimental conditions were determined based on the results from the method assessment experiments as follows: for ethane, samples were incubated with 2 μCi (140 nM) for 12 hours near *in situ* temperature; for propane, samples were incubated with 1 μCi (50 nM) for 24 hours near *in situ* temperature; for butane, samples were incubated with 2 μCi (35 nM) for 24 hours near *in situ* temperature (Table 3). Each replicate was injected with 100 μL of diluted tracer (a mixture of tritiated stock and N_2 gas), allowing for consistent and reproducible injections across replicate bottles. Ethane, propane, and butane diluted stock concentrations were 0.02 Ci/L, 0.01 Ci/L, 0.02 Ci/L, respectively.

3. Results

3.1 Tracer Synthesis and Chemical Stability (Phase 1)

Tritiated ethane, propane, and butane were successfully synthesized using tritiated water and ethylmagnesium bromide, propylmagnesium chloride, and butylmagnesium bromide. Percent yields of tritiated gas were calculated with reference to tritiated water substrate and specific activity of synthesis gas was quantified in Ci/L and converted to mCi per mmole of hydrocarbon (Table 3).

Following synthesis, the tracers were stored individually over an aqueous brine solution, which led to an increase of radioactivity in the aqueous solution over time, presumably because of hydrogen exchange between each hydrocarbon and water [Bottinga, 1969; Horibe and Craig, 1995]. Isotope exchange also occurs with storage of tritium-labeled methane and is likely catalyzed by radicals formed following the autoradiolytic cleavage of C-T bonds. The gradual loss of tracer activity to the aqueous phase during storage combined with tritium's half-life of 12.3 years limits the useful lifetime of any batch of tracer to a period of <10 years. To correct for the influence of abiotic exchange during use of the tracer, kill controls are needed to empirically determine the amount of tritium incorporated into the seawater in the absence of microbial consumption. Tracer activity was assessed regularly by methods described above to ensure that the injected tracer quantity is correct. A bias in tracer concentration will propagate through equation 13 and yield an incorrect rate. Transfer and purification of the tracer stock is also recommended when the stock has gone unused for a period of several months.

3.2 Method Assessment (Phase 2)

The tritiated tracer oxidation rate method was tested with water collected at a single station in September, 2011 (Table 1). Each hydrocarbon tracer was evaluated for microbial response by varying: (1) the quantity of tritium-labeled substrate in the sample (i.e., activity), (2) the length of time for which each individual sample was incubated (i.e., incubation time), and (3) the temperature at which the sample was incubated (i.e., temperature**)**. This ^{3}H tracer method was also compared to a previously utilized ^{13}C method [*Valentine et al*., 2010]. Results from the method assessment experiments are shown in Figures 3, 4, and 5. Methane had a fractional turnover rate of 9.6×10^{-4} d^{-1} (turnover time of ~3 years) and an oxidation rate of 2.0 nM d^{-1}, while ethane, propane, and butane had fractional turnover rates of 0.24, 0.17, and 0.71 d^{-1} (turnover times of ~4, 6, and 1.5 days), respectively, and oxidation rates of 20, 8.7, and 7.1 nM day^{-1}, for the same incubation conditions. For reference, samples subjected to an incubation period of 24 hours have a maximum measurable fractional turnover rate of 1 d^{-1}; for samples subject to an incubation period of 12 hours, the maximum measurable fractional turnover rate is 2 d^{-1} (i.e., complete substrate consumption after the incubation period).

3.2.1 Kill Controls

Control experiments were conducted by treating a subset of samples with saturated mercuric chloride to halt biological activity. Comparing killed to non-killed samples, only a small amount of product is generated by abiotic reactions (Figure 6). Any activity found in the kill controls can thus be subtracted out as baseline and attributed to abiotic tritium exchange.

3.2.2 Activity

For ethane, the fractional turnover rate increased with increasing activity of tracer, most notably between the 1 and 2 μCi treatments. A discrepancy between duplicate samples treated with 4 μCi of tracer does not allow differentiation between two possible trends (Figure 3A): a continued linear increase in the fractional turnover rate with added tracer or a plateau in the turnover rate above 2 μCi. A linear increase is consistent with bacterial adaptation or growth, whereas a plateau is consistent with first order kinetic behavior. Based on these results, samples were incubated with 2 μCi of ethane for subsequent application of the method. 2 μCi was chosen to provide both a consistent response and a measureable level of tritium in the metabolic products.

Propane and butane fractional turnover rates increased linearly when tracer was varied from 1 to 2 μCi and 1 to 4 μCi, respectively, with the exception of duplicates at 2 μCi for butane (Figure 3B, 3C). This linear behavior is reflective of an adaptive response, suggesting that increasing levels of tracer affected the metabolic capacity of the community. Fractional turnover rate reached a maximum of 0.35 d^{-1} for propane and 0.05 d^{-1} for butane, except for butane's duplicate outlier that exceeded 0.1 d^{-1}. Divergence in the fractional turnover rate occurred at tracer additions $\geq$ 2 μCi. The molar quantity of tracer needed to achieve these activities was 12 fold greater than the ambient concentration, and the variability may represent inherent differences in growth or adaptive response. Based on these results we opted to incubate samples with 1 μCi of propane or 2 μCi of butane for

subsequent applications of these methods. These quantities of tracer were chosen to provide measureable levels of tritium in the metabolic products.

A comparison of fractional turnover rate versus concentration for each hydrocarbon (Figure 3D) indicates an exponential relationship between the concentration and fractional turnover rate for each substrate, which is consistent with an adaptive response by the microbial community. These results further indicate that the microbial communities responded to the addition of ethane, propane, and butane, even at concentrations less than 50, 270, and 20 nM, respectively (Figure 3D).

3.2.3 Incubation Time

The fractional turnover rate for ethane increased exponentially over the course of 24 hours (Figure 4A), presumably reflecting adaptation by the microbial population. After incubation for 24 hours, the fractional turnover rate for ethane reached a value of 0.85 d^{-1}, approaching the empirical limit for this method. This exponential trend can be attributed to either of two distinct environmental factors: (1) an artificial response due to the added tracer, or (2) population growth due to the naturally high ethane concentration introduced at the Coal Oil Point seeps. We favor a combination of these explanations wherein the microbial community began growing exponentially following exposure at Coal Oil Point and the addition of tracer prolonged this exponential phase. Based on the rapid adaptation for ethane, we opted to incubate samples for a period of 12 hours for subsequent applications of this method. This period of time was viewed as being sufficient to generate measureable

levels of tritium in the metabolic products, but not so long as to stimulate complete consumption.

The time-course change in fractional turnover rates for propane and butane were distinctive compared to ethane. Both displayed decreases between 6 and 12 hours of incubation, which is opposite the trend observed for ethane. Following 12 hours of incubation, the fractional turnover rate for propane remained relatively constant or decreased slightly through the termination of the experiment at 48 hours (Figure 4B). Butane's fractional turnover rate gradually increased during the time interval from 12 to 48 hours (Figure 4C). Based on these results for propane and butane, we opted to incubate samples for a period of 24 hours for subsequent applications of this method.

The cause of the divergent trends for ethane versus propane and butane is not immediately apparent. Figure 4D highlights the coincidence in timing between the depletion of ethane and the increase in rate of consumption for propane and butane. While speculative, this timing is consistent with co-metabolism of propane and butane by ethane-consuming bacteria.

3.2.4 Temperature

The impact of temperature on the fractional turnover rates for ethane, propane, and butane was assessed by incubating samples at 0, 4, 11, and 20 °C, bracketing the ambient temperature of 11.5 °C. The fractional turnover rate was found to increase with temperature

in this range, for all treatments (Figure 5). The observed trends are typical for a marine microbial community and likely reflect a metabolic response to temperature.

3.2.5 ^{13}C Tracer and Substrate Concentration

A comparison of oxidation rates measured using the tritium method and ^{13}C-labeled ethane and propane revealed concentration dependence (Figures 7 and 8). A direct comparison between the two methods was hampered by this effect as the detection limit for ^{13}C in metabolic products required substrate concentrations from 3.3 to 30 μM, far above the ambient levels. The observed maximum oxidation rate occurred at tracer concentrations of 2.9 - 7.1 μM for both ethane and propane. Surprisingly, the oxidation rate decreased with increasing concentration beyond these maxima. This might suggest some form of inhibition at elevated substrate concentration. Alternatively, the two methods measure different metabolic products. The ^{3}H method measures all ^{3}H remaining in the sample, including the final product ($^{3}H_2O$) and all soluble ^{3}H-intermediates. The ^{3}H method, in effect, measures the rate of hydrocarbon loss in a sample, rather than the rate of product formation, whereas the ^{13}C method quantifies only the final carbon species of the oxidation pathway (CO_2). Results from the ^{13}C tracer application are consistent with a rate of incomplete metabolism or biomass accumulation that increases with substrate concentration in this range.

3.3 Tracking the Hydrocarbon Plume from Coal Oil Point (Phase 3)

The oxidation of ethane, propane, and butane was studied in the Santa Barbara Channel, within the down-current plume of a hydrocarbon seep, in order to assess the *in situ* response of the marine microbial community to the input of these gases. This setting also

provided context to the method assessment described above, during which all water had been collected at one location in this plume (station Plume 3). Monitoring currents with HF radar enabled tracking of hydrocarbon-laden waters from the seep field to a distance of 33 km down-current, at which point plume features were lost (Figure 2; Table 2). Methane was used to track the plume as its oxidation occurred slowly relative to the transit time of the water and no major seeps are known along the plume's path. Turnover time for methane was ~3 years compared to 3 days for the water to travel 33 km. Thus, methane was treated as a conservative tracer for hydrocarbon exposure.

Currents exhibited a counterclockwise rotation on all sampling days in the study area, common for the Santa Barbara Channel (Figure 2) [*Harms and Winant*, 1998]. As a result of this cyclonic motion, the dissolved hydrocarbon plume located on the north side of the basin traveled westward. The travel time between Coal Oil Point and stations within the dissolved plume were calculated by dividing the distance traveled by the current velocity. Current velocities taken during sampling intervals averaged 11.8 km/d (0.14 m/s ± 0.05 m/s), which is consistent with previous studies [*Beckenbach*, 2004]. The travel time of water from the Coal Oil Point seep field to each station is expressed here in terms of time since exposure (TSE) using the average current velocity, as this term provides a clear metric for comparison to microbial adaptation. Note however that stations were sampled on different days and the results are not a true time-series.

3.3.1 Hydrocarbon Gas Concentrations within the Plume

The highest concentrations of ethane, propane, and butane (1750 nM, 570 nM, and 400 nM, respectively) were measured in samples collected at Coal Oil Point (station Plume 2). Concentrations generally decreased as the plume travelled with the current. Ethane, propane, and butane were no longer detectable (<1.5 nM) 1.5 days following exposure. Mixing within the plume samples was determined based on methane concentrations. Methane was considered to be a conservative tracer, oxidation rates observed were very low (turnover time of ~3 years), and the plume was located below the mixed layer depth [*Mau et al*., 2007]. Methane concentrations were variable within the plume (Table 2). In some cases, samples collected down-current were more concentrated in methane than samples collected further up current. This behavior is expected for spot sampling of a dynamic feature and likely indicates the complexity in current flow and mixing. By treating methane as a conservative tracer, we were able to track the relative declines in ethane, propane, and butane (Figures 9C, 10C and 11C), which we attribute to oxidation by bacteria in the plume. These results indicate that > 99% of the ethane, propane, and butane was consumed within 1.3 days of exposure.

3.3.2 Fractional Turnover Rate within the Plume

The impact of exposure on the fractional turnover rate was similar for each of the three gases tested (Figures 9A, 10A, and 11A). Low rates at the time of initial exposure gave way to higher rates down-current, and then decreased back to low rates following substrate depletion. Ethane consumption occurred more rapidly than propane and butane consumption, reaching a maximum in samples collected 1.25 days following exposure, with

a fractional turnover rate ≥2 d^{-1}. That is, 30 hours following initial exposure, the microbial community was able to consume the entirety of added ethane tracer within a period of 12 hours. Rates decreased down-current in the absence of elevated ethane concentration until negligible tracer was removed from samples collected 2.75 days following initial exposure. This form of decay in the time course of activity may reflect both physical dilution of the microbial population and the response of the microbial community to ethane deprivation. Similarly, propane and butane consumption rates reached their maximums in samples collected 1.8 days following exposure, and then decreased down-current. The maximum rate of tracer removal was 0.89 d^{-1} for propane, while butane's fractional turnover rate never exceeded 0.2 d^{-1}. Butane consumption was sustained over the greatest time span with rates of tracer consumption averaging ~0.05 d^{-1} in samples collected 0.75 - 2.75 days following exposure. These results demonstrate that at Coal Oil Point, ethane, propane, and butane are consumed by the indigenous bacterial community within 2-3 days following exposure.

4. Discussion

4.1 Oxidation Rates and Kinetic Order

Conversion of radioisotope tracers as substrate to product is commonly used to estimate the rate of metabolism for a given set of conditions. The method described in this work is similar to that used for quantifying methane oxidation rates [*Mau et al*., 2013; *Valentine et al*., 2001; *Ward et al*., 1987], wherein the transfer of tritium from methane to the aqueous phase is quantified following the incubation of a representative sample of

seawater at conditions that approximate those experienced *in situ* by the microbial community. In the case of methane oxidation rate measurements, the low concentration of added methane (on the order of 10 nM) does not typically elicit a response in the microbial community [*Pack et al*., 2011; *Ward et al*., 1987] and is thus assumed to reflect the *in situ* rate of consumption. The results presented here demonstrate that microbial communities adapt more rapidly to the input of ethane, propane, or butane and require different treatments of the resulting data.

Results from the method assessment demonstrate that the quantity of tracer injected and the duration of the incubation impact the fractional turnover rate calculated from the incubations. These results violate the assumptions outlined in Section 2.2.4 (Calculating Oxidation Rates) and illustrate several important differences between methane oxidation versus that of ethane, propane, and butane. First, the microbial community displays a clear adaptive response to the input of substrate wherein the addition of substrate primes metabolic rate (Figure 3). Second, ethane consumption by the microbial community displays an exponential rise during 24 hour incubations (Figure 4A). This trend indicates rapid adaptation, though the data does not distinguish between the input of ethane at the seep versus the added tracer. Third, inconsistency in the trends observed for propane and butane (Figures 3 and 4) may relate to the fate of ethane introduced naturally from the seeps. Adaptation to ethane occurred rapidly compared to propane and butane. A substrate specificity that encompasses ethane, propane, and butane might explain the variability in the time course of propane and butane oxidation (Figures 4B and 4C). Given indications of an

adaptive bacterial response to substrate input, we have not interpreted the results using a purely kinetic model. However, the results presented in Figures 7A and 8A indicate that the Michaelis-Menten model may aptly describe the rate's substrate response, for select experimental conditions. Interestingly, such an analysis indicates a first order response to ethane and propane, but a zero-order response to butane.

Results from plume tracking studies are consistent with those from the method assessment. The microbial community adapted to consume ethane, propane, and butane within ~1 day following exposure. This timescale frames the method assessment in a way that was not intended, in that samples used to assess the method were exposed to hydrocarbons on a similar time frame, indicating they may have been actively adapting to the hydrocarbon input at the time of sampling. Nonetheless, both the method assessment and the plume tracking studies reveal the same important trend: microbial adaptation to the input of ethane, propane, and butane occurs rapidly in this environment.

The rapid adaptive response of microbes to the input of ethane, propane, and butane limits the utility of kinetic expressions to describe the *in situ* rate of metabolism. Rates of hydrocarbon oxidation measured using isotope tracers are typically expressed as an *in situ* rate, a potential rate, or with a model such as Michaelis-Menten. The *in situ* rates are calculated as described in equation 13, and typically assume adherence to first order kinetic behavior. Potential rates are calculated from conditions of elevated substrate concentration, at the point that the rate transitions to become zero order [*Reeburgh*, 1983; *Valentine et al*., 2010]. However, none of these kinetic behaviors accurately reflect an actively adapting or

growing microbial community, which is expected to display an exponential increase in the rate of metabolism as the population of consumers increases.

Based on the results, we find the utility of oxidation rate measurements for ethane, propane, and butane to be restricted compared to those for methane. In the case of methane, such measurements are typically indicative of the microbes' *in situ* metabolic rate, and are thus useful for calculating methane budgets under steady-state conditions. For ethane, propane, and butane, such measurements are more indicative of the microbial communities' capacity to respond to the input of substrates into the environment. This distinction is rooted in the fundamentally more rapid response of ethane, propane, and butane degraders to the input of substrate when compared to methane degraders. Fractional turnover rate calculated from these tracer experiments provide a conservative representation of the *in situ* microbial condition, based on the expectations of kinetic models such as Michaelis-Menten.. Further, given that the threshold concentrations for consumption of methane is higher by a factor of ten or more compared to ethane, propane, and butane, a more sensitive tracer method would be needed to calculate *in situ* rates for ethane, propane, and butane consumption at steady-state conditions. The use of a higher-activity tritium-label or a low-level ^{14}C tracer coupled with accelerator mass spectrometry are two potential approaches to limit the amount of additional substrate needed to calculate a rate measurement [*Pack et al*., 2011].

4.2 Fate of Hydrocarbons in the Coal Oil Point Plume

Ethane, propane, and butane are oxidized more rapidly than methane, thus the concentration of methane within the plume decreases more slowly than that of the other

gases. By comparing the ratio of ethane/methane, propane/methane, and butane/methane, a shift toward methane is indicative of preferential microbial consumption [*Kinnaman et al*., 2007; *Valentine et al*., 2010]. Methane becomes more dominant as the plume travels down-current, consistent with previous geochemical observations in the Santa Barbara Channel [*Clark et al*., 2000; *Mau et al*., 2007] (Figures 9C, 10C, and 11C). This trend is well supported by the rapid consumption rates observed within the plume (Figures 9D, 10D, and 11D).

Microbial response to the hydrocarbon plume emanating from Coal Oil Point shows the community's increased activity due to elevated substrate followed by a decrease due to substrate limitation. While substrates are still present within the plume, microbial consumption rates increase as hydrocarbon concentration decreases. As the plume ages and hydrocarbon concentrations fall below detection, fractional turnover rates began to drop. The longer the plume sustained hydrocarbon starvation, the lower the fractional turnover rates became. Even though all three gases had similar trends and reached their maximum consumption rate at 1.25 days, each gas maintained its maximum rate for a different duration (~1.25 days travel time for ethane, ~1.8 days for propane, ~2.5 days for butane; Figures 9, 10, 11). Ethane was consumed more quickly than propane or butane, which contrasts deep ocean samples and laboratory incubations that observed more rapid propane consumption compared to ethane [*Kinnaman et al*., 2007; *Redmond and Valentine*, 2010].

4.3 Microbial Adaptation to Hydrocarbons

Data presented in the method assessment showed that ethane had a fractional turnover rate which increased exponentially over a 24 hour period. This suggests that microbial growth was occurring over the course of the incubation (Figure 4A). This could be an artificial response to the added tracer or a population growth response to the naturally high hydrocarbon levels introduced at the Coal Oil Point seep. Samples for the method assessment experiment were collected 13 km from the plume's origin. Fractional turnover rates in the plume's water show that rates progressive increase as the water moves down-current until reaching ~15.5 km (Figure 9A). Samples for the method assessment were collected down current from the observed maximum, and assuming similar current velocities and water mixing at the different times, we predict that microbial growth was likely due to the environmental response to the natural seep and not exclusively to the addition of tracer.

Hydrocarbon consuming organisms typically make up a small fraction of the total open ocean bacterial community; however, when substrates are available, they can grow to dominate the community [*Harayama et al*., 1999; *Margesin and Schinner*, 1999; *Redmond and Valentine*, 2012]. Only two studies have identified aerobic oxidizers of ethane and propane in marine environments [*Redmond et al*., 2010; *Redmond and Valentine*, 2012]. In laboratory incubations with sediment collected near a natural thermogenic seep, *Redmond et al*. [2010] observed that ethane was primarily consumed by a group of organisms from the family Methylococcaceae, closely related to, but distinct from, the methane oxidizing Methylococcaceae observed in the same samples. Propane was primarily consumed by members of an unclassified Gammaproteobacterial group and was consumed more slowly

than methane or ethane. In contrast, propane was oxidized more rapidly than ethane in hydrocarbon plumes formed during the 2010 Gulf of Mexico oil spill [*Valentine et al*., 2010]. Both ethane and propane were initially consumed more rapidly than methane, though methane oxidation rates eventually increased enough that nearly all of the methane was consumed by bacteria [*Kessler et al*., 2011; *Du and Kessler*, 2012]. Methylococcaceae were the dominant methane oxidizers, while ethane and propane oxidation was driven predominately by Colwellia [*Redmond and Valentine,* 2012].

Hydrocarbon oxidation in the Coal Oil Point water column is similar to the oil spill scenario in that ethane and propane oxidation increased more rapidly than methane oxidation following exposure. The present Coal Oil Point study differs in that ethane was oxidized more rapidly than propane. This may have been due to more rapid growth by ethane oxidizers or to substrate preferences in bacteria that could oxidize ethane, propane, and butane. The much lower rates of methane oxidation suggest that this process was performed by other, slow-growing bacteria.

Since little is known about bacterial populations that consume ethane, propane, and butane in natural marine systems, we estimated the potential bacterial production from consumption of these hydrocarbons within the Coal Oil Point plume. Estimates of bacterial growth efficiencies are based on the reported range of 5% to 65% for aerobic methanotrophs since equivalent data is sparse for consumers of ethane, propane and butane. [*Griffiths et al*., 1982; *Ward et al*., 1987]. Production estimates for the 6 stations with rates above background are shown in Figure 12A. The low end estimates ranged between 0.0011 $x10^{-6}$

mol C $L^{-1}d^{-1}$ and $0.12x10^{-6}$ mol C $L^{-1}d^{-1}$, while the high end estimates ranged between 0.014 $x10^{-6}$ mol C $L^{-1}d^{-1}$ and $1.7x10^{-6}$ mol C $L^{-1}d^{-1}$. In comparison, ^{3}H-Leucine incorporation measurements of net bacterial production in Santa Barbara Channel surface waters (35-55 m) typically range between 0.1 $x10^{-6}$ to 0.8 $x10^{-6}$ mol C $L^{-1}d^{-1}$ (Data courtesy of Craig Carlson and Emma Wear). Our estimates indicate that that microbial production from hydrocarbon oxidation in the plume are equivalent to ~1 % to ~213% of background microbial production. Similarly, the total bacterial biomass produced within the plume was calculated using a moving average approach for both the low and high end net bacterial production estimates (Figure 12B). A carbon conversion factor of 15 fg C $cell^{-1}$ was used [*Halewood et al*., 2012]. Assuming no loss of cells as the plume travels down current, biomass accumulation within the plume ranges from 5.8 $x10^{7}$ cell $L^{-1}$to 7.6 $x10^{8}$ cell L^{-1}, indicating that a rapid bloom of hydrocarbon-degrading bacteria that could account for up to ~68% of the microbial community in the affected waters, at-least transiently.

5. Conclusion

Development of methods to quantify bacterial consumption of ethane, propane and butane revealed a rapid and dynamic microbial response to hydrocarbon exposure, down current from a natural gas seep. The complete consumption of ethane, propane and butane within 3-days of exposure is far more rapid than would be predicted based upon methane's behavior, and highlights the important distinction between the biogeochemistry of methane and other hydrocarbon gases. Significant gaps remain in our understanding of the environment's response to an irruption of natural gas that include the identities, physiologies

and distributions of major consumers; however, this work confirms our previous observation [*Valentine et al*., 2010] as to the Ocean's potential for a rapid microbial response.

Acknowledgements:

Sampling and experimental efforts were aided by Christoph Pierre, Christian Orsini, David Salazar, Avi Rubin, Ryan Duncombe, as well as the Captain and crew of the *R/V Atlantis* during the SEEPS-11 expedition. Georges Paradis conducted stable isotope analyses, and Emma Wear and Craig Carlson provided bacterial production data. Contact corresponding author David Valentine to request any data. Funding for this work was provided by National Science Foundation, grants OCE-0961725 and OCE-1155855, to DLV. SDM was funded by a Ford Foundation Predoctoral Fellowship.

References:

Adams, M. M., A. L. Hoarfrost, S. Bose, S. B. Joye, P. R. Girguis (2013), Anaerobic oxidation of short-chain alkanes in hydrothermal sediments: potential influences on sulfur cycling and microbial diversity, *Frontiers in Microbiology*, 4. doi:10.3389/fmicb.2013.00110

Arp, D. J. (1999), Butane metabolism by butane-grown 'Pseudomonas butanovora', *Microbiology*, 145(5), 1173-1180.

Ashraf, W., A. Mihdhir, and C.J. Murrell (1994), Bacterial oxidation of propane. *FEMS Microbiology Letters*, 122(1), 1-6.

Beckenbach, E. (2004), Surface circulation in the Santa Barbara Channel: An application of high frequency radar for descriptive physical oceanography in the coastal zone, Ph.D. thesis, Univ. of California, Santa Barbara.

Bottinga, Y. (1969), Calculated fractionation factors for carbon and hydrogen isotope exchange in the system calcite-carbon dioxide-graphite-methane-hydrogen-water vapor, *Geochim Cosmochim Acta*, 33(1), 49-64.

Cicerone, R. J. and R.S. Oremland (1988), Biogeochemical aspects of atmospheric methane. *Global Biogeochemical Cycles*, 2(4), 299-327.

Clark, J., L. Washburn, J. S. Hornafius, and B. P. Luyendyk (2000), Dissolved hydrocarbon flux from natural marine seeps to the southern California Bight, *Journal Geophysical Research*, 105(C5), 11,509–11,522.

Collins, W., R. Derwent, C. Johnson, and D. Stevenson (2002), The oxidation of organic compounds in the troposphere and their global warming potentials, *Climatic Change*, 52: 453–479.

Etiope, G., K. R. Lassey, R. W. Klusman, and E. Boschi, (2008), Reappraisal of the fossil methane budget and related emission from geologic sources, *Journal of Geophyiscal Research*, 35(9), doi:10.1029/2008GL033623.

Fung, I., J. John, J. Lerner and E. Matthews, M. Prather, L. P. Steele, P. J. Fraser (1991), Three-dimensional model synthesis of the global methane cycle, *Journal of Geophysical Research.* 96, 12033–12065.

Griffiths, R.D., B.A. Caldwell, J.D. Cline, W.A. Broich, R.Y. Morita (1982), Field observations of methane concentrations and oxidation rates in the southeastern Bering Sea, *Applied and Environmental Microbiology*, 44, 436–446.

Coast Guard, United States (2013), Oil Pollution Act Liability Limits in 2013, 1-28.

Du, M., and J.D. Kessler (2012), Assessment of the spatial and temporal variability of bulk hydrocarbon respiration following the Deepwater Horizon oil spill. *Environmental Science & Technology*, 46(19), 10499-10507.

Halewood, E.R., C.A. Carlson, M.A. Brzezinski, D.C. Reed, and J. Goodman (2012), Annual cycle of organic matter partitioning and its availability to bacteria across the Santa Barbara Channel continental shelf, *Aquatic Microbial Ecology*, 67:189–209.

Hanson, R.S., and T.E. Hanson (1996), Methanotrophic bacteria. *Microbiological Reviews*, 60(2), 439-471.

Harayama, S., H. Kishira, Y. Kasai, and K. Shutsubo (1999), Petroleum biodegradation in marine environments. *Journal of Molecular Microbiology and Biotechnology*, 1(1), 63-70.

Harms, S., and C.D. Winant (1998), Characteristic patterns of the circulation in the Santa Barbara Channel, *Journal of Geophysical Research*, 103(C2), 3041–3065.

Heintz, M.B., S. Mau, and D.L. Valentine (2012), Physical control on methanotrophic potential in waters of the Santa Monica Basin, Southern California, *Limnology and Oceanography*, 57(2), 420-432, doi:10.4319/lo.2012.57.2.0420.

Horibe, Y., and H. Craig (1995), DH fractionation in the system methane-hydrogen-water, *Geochim Cosmochim Acta*, 59(24), 5209-5217.

Hornafius, J.S., D.C. Quigley, and B.P. Luyendyk (1999), The world's most spectacular marine hydrocarbon seeps (Coal Oil Point, Santa Barbara Channel, California): Quantification of emission, *Journal of Geophysical Research*, 104(C9), 20,703– 20,711.

Jacob, D.J., B.D. Field, E.M. Jin, I. Bey, Q. Li, J.A. Logan, R.M. Yantosca, and H.B. Singh (2002), Atmospheric budget of acetone. *Journal of Geophysical Research: Atmospheres*, 107(D10), ACH-5.

Joye, S.B., T.L. Connell, L.G. Miller, R.S. Oremland, and R.S. Jellison (1999), Oxidation of ammonia and methane in an alkaline, saline lake. *Limnology and oceanography*, 44(1), 178-188.

Katzenstein, A.S., L.A. Doezema, I.J. Simpson, D.R. Blake, and F.S. Rowland (2003), Extensive regional atmospheric hydrocarbon pollution in the southwestern United States, *Proceedings of the National Academy of Sciences*, 100(21), 11975-11979.

Kessler, J.D., D.L. Valentine, M.C. Redmond, M. Du, E.W. Chan, S.D. Mendes, E.W. Quiroz. et al. (2011), A persistent oxygen anomaly reveals the fate of spilled methane in the deep Gulf of Mexico. *Science*, (6015) 312-315.

Kinnaman, F.S., D.L. Valentine, and S.C. Tyler (2007), Carbon and hydrogen isotope fractionation associated with the aerobic microbial oxidation of methane, ethane, propane and butane, *Geochim Cosmochim Acta*, 71, 271–283.

Margesin, R., and F. Schinner (1999), Biological decontamination of oil spills in cold environments, *Journal of Chemical Technology and Biotechnology*, 74(5), 381-389.

Mastalerz, V., G.J. De Lange, and A. Dählmann (2009), Differential aerobic and anaerobic oxidation of hydrocarbon gases discharged at mud volcanoes in the Nile deep-sea fan, *Geochim Cosmochim Acta*, 73(13), 3849-3863.

Mau, S., J. Blees, E. Helmke, H. Niemann, and E. Damm (2013), Vertical distribution of methane oxidation and methanotrophic response to elevated methane concentrations in stratified waters of the Arctic fjord Storfjorden (Svalbard, Norway), *Biogeosciences*, (10), 6267-6278.

Mau, S., M.B. Heintz, F.S. Kinnaman, and D.L. Valentine (2010), Compositional variability and air-sea flux of ethane and propane in the plume of a large, marine seep field near Coal Oil Point, CA, *Geo-Marine Letters*, 30(3-4), 367-378.

Mau, S., D.L. Valentine, J.F. Clark, J. Reed, R. Camilli, and L. Washburn (2007), Dissolved methane distributions and air‐sea flux in the plume of a massive seep field, Coal Oil Point, California. *Geophysical Research Letters*, 34(22). doi:10.1029/2007GL031344.

Olszowy, H. and W. Kitching (1984), Stereochemistry of trifluoroacetolysis and brominolysis of the cyclohexyl-tin bond, *Organometallics*, 3(11), 1676-1683.

Pack, M.A., M.B. Heintz, W.S. Reeburgh, S.E. Trumbore, D.L. Valentine, X. Xu, and E.R. Druffel (2011), A method for measuring methane oxidation rates using low-levels of 14C-labeled methane and accelerator mass spectrometry. *Limnology and Oceanography: Methods*, 9, 245-260.

Perry, J. (1980), Propane utilization by microorganisms, *Advances in Applied Microbiology*, 26, 89-115.

Plass-Dulmer, C., R. Koppmann, M. Ratte, and J. Rudolph (1995), Light nonmethane hydrocarbons in seawater, *Global Biogeochemical Cycles*, 9(1), 79-100.

Quistad, S.D., and D.L. Valentine (2011), Anaerobic propane oxidation in marine hydrocarbon seep sediments, *Geochim Cosmochim Acta*, 75(8), 2159-2169.

Reddy, C.M., J.S. Arey, J.S. Seewald, S.P. Sylva, K.L. Lemkau, R.K. Nelson, C.A. Carmichael, C.P. McIntyre, J. Fenwick, G.T. Ventura, B.A.S. Van Mooy, and R. Camilli (2012), Composition and fate of gas and oil released to the water column during the Deepwater Horizon oil spill. *Proceedings of the National Academy of Sciences*, 109(50), 20229-20234.

Redmond, M.C., and D.L. Valentine (2012), Natural gas and temperature structured a microbial community response to the Deepwater Horizon oil spill, *Proceedings of the National Academy of Sciences*, 109(50), 20292-20297. doi:10.1073/pnas.1108756108

Redmond, M.C., D.L. Valentine, and A.L. Sessions (2010), Identification of novel methane-, ethane-, and propane-oxidizing bacteria at marine hydrocarbon seeps by stable isotope probing. *Applied and Environmental Microbiology*, 76(19), 6412-6422.

Reeburgh, W.S. (1969). Observations of gases in Chesapeake Bay sediments. *Limnololgy and Oceanography*, 14(3), 368-375.

Reeburgh, W.S. (1983), Rates of biogeochemical processes in anoxic sediments, *Annual Review of Earth and Planetary Sciences*, 11(1), 269-298.

Reeburgh, W.S. (2007), Oceanic methane biogeochemistry, *Chemical Reviews*, 107, 486–513.

Reeburgh, W.S., B.B. Ward, S.C. Whalen, K.A. Sandbeck, K.A. Kilpatrickt, and L.J. Kerkhof (1991), Black Sea methane geochemistry. *Deep Sea Research Part A. Oceanographic Research Papers*, 38, S1189-S1210.

Singh, H.B., D. O'hara, D. Herlth, W. Sachse, D.R. Blake, J.D. Bradshaw, M. Kanakidou and P.J. Crutzen (1994), Acetone in the atmosphere: Distribution, sources, and sinks. *Journal of Geophysical Research: Atmospheres*, 99(D1), 1805-1819.

Valentine, D.L. (2011), Emerging topics in marine methane biogeochemistry, *Annual Review of Marine Science*, 3(1), 147-171. doi:10.1146/annurev-marine-120709-142734

Valentine, D.L., J.D. Kessler, M.C. Redmond, S.D. Mendes, M.B. Heintz, C. Farwell, L. Hu, F.S. Kinnaman, S. Yvon-Lewis, M. Du, E.W. Chan, F.G. Tigreros, and C.J. Villanueva (2010), Propane respiration jump-starts microbial response to a deep oil spill, *Science*, 330(6001), 208-211. doi:10.1126/science.1196830

Valentine, D.L., D. Blanton, W.S. Reeburgh, and M. Kastner (2001), Water column methane oxidation adjacent to an area of active hydrate dissociation, Eel River Basin, *Geochim Cosmochim Acta*, 65(16), 2633-2640.

Ward, B.B., K.A. Kilpatrick, P.C. Novelli, and M.I. Scranton (1987), Methane oxidation and methane fluxes in the ocean surface layer and deep anoxic waters, *Nature*, 327(6119), 226-229.

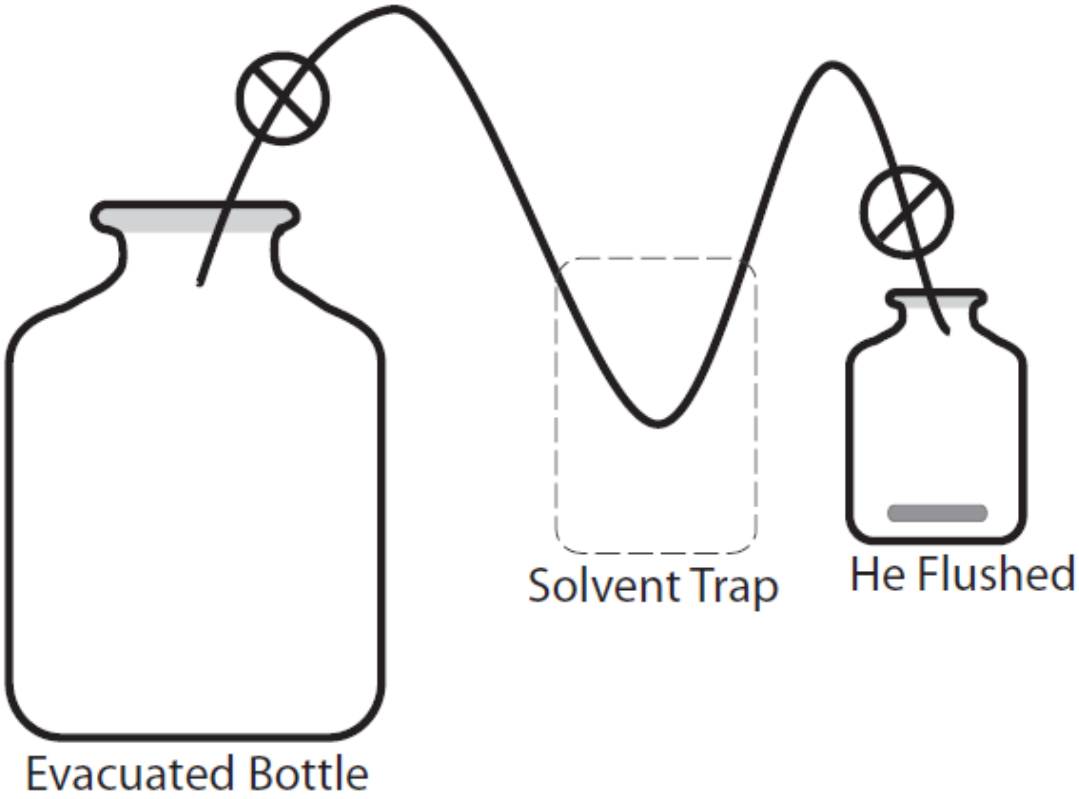

Figure 1. Schematic for synthesis of tritium labeled hydrocarbon gases. The synthesis occurred in the He flushed reaction bottle and any gas produced was transferred to an evacuated collection bottle. The solvent trap (dry ice and acetone) was used to remove any residual organic solvent or water from the synthesized gas.

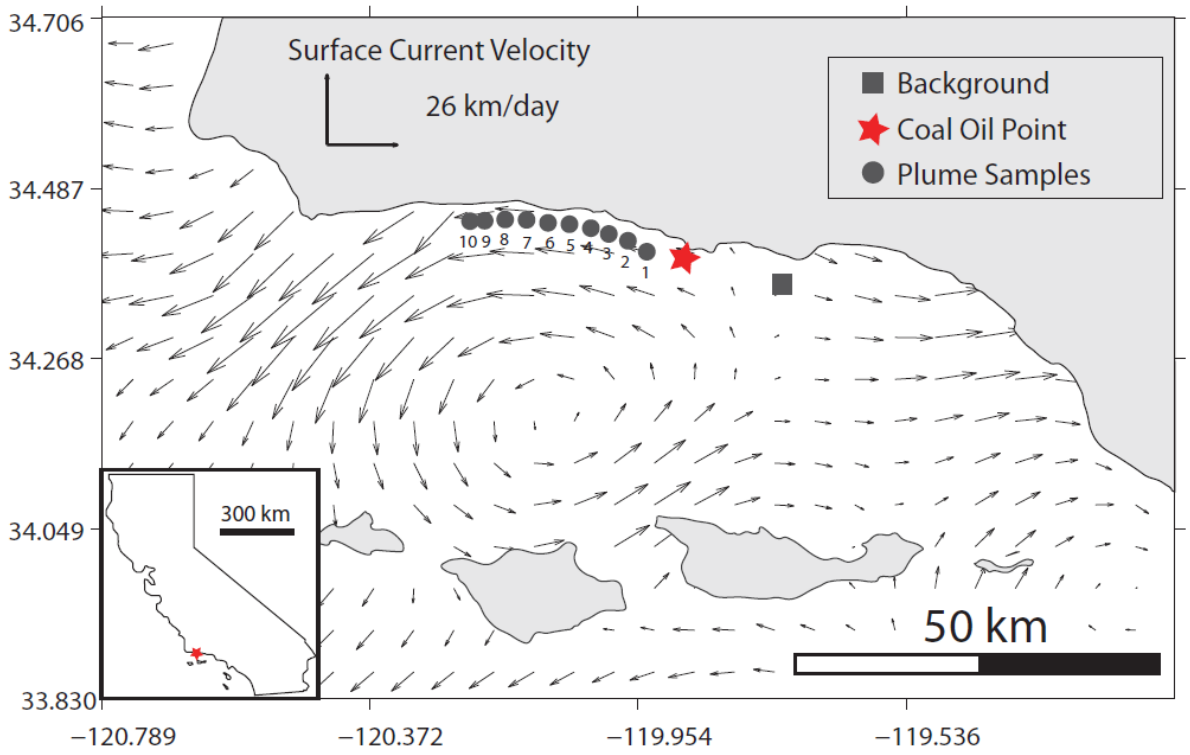

Figure 2. The Coal Oil Point seep field (represented by the red star) is located off-shore Goleta, California. Arrows represent surface current velocities averaged during the plume sampling period from July 23, 2012 to September 25, 2012. The background sample (represented by the gray square) was collected outside of the seep area on September 16, 2011.

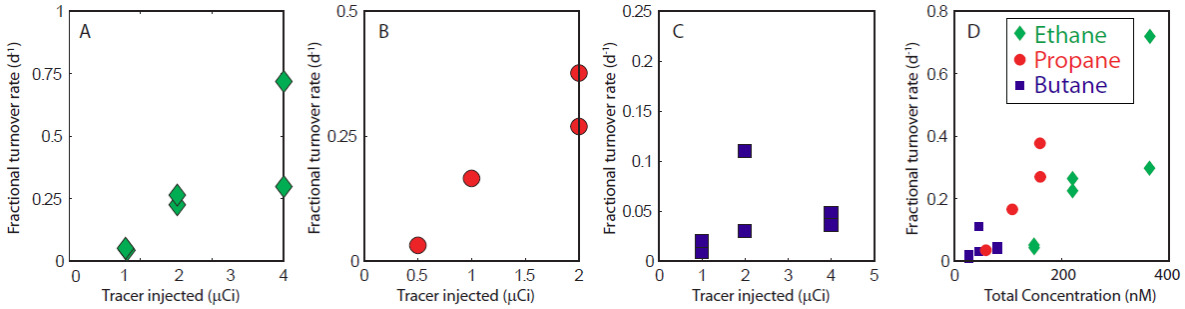

Figure 3. Response of the microbial community to addition of different quantities of tracer: A) ethane B) propane; and C) butane. D) Total concentration of gas in bottle versus fractional turnover rate. All treatments were incubated at 11°C for 24h. Duplicates are shown for each quantity of tracer injected, but some are too similar to be visually distinguished.

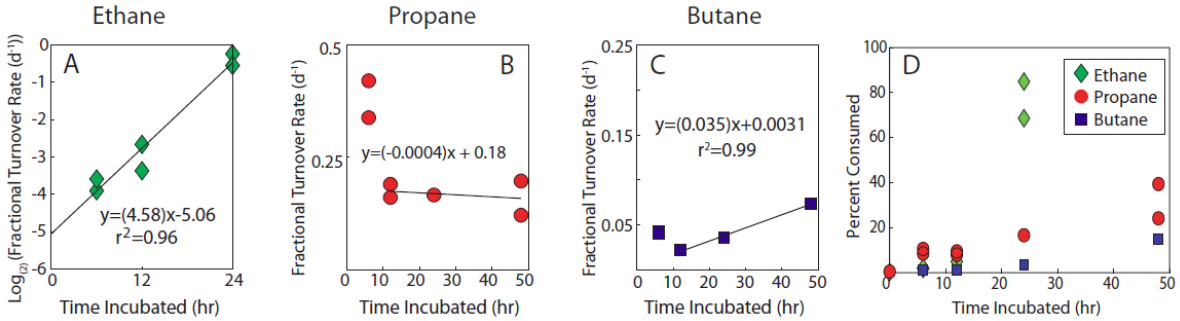

Figure 4. Incubation time response experiment conducted as part of the method assessment for A) Ethane: incubated at 11 °C with 2 µCi of tracer. B) Propane: incubated at 11°C with 1 µCi of tracer, and C) Butane: incubated at 11°Cwith 2 µCi of tracer. D) Incubation time series for ethane, propane, and butane showing the percent of tracer converted at different incubation times. Duplicates are shown for each sample interval. Regression in panels B and C exclude the 6 hr time point.

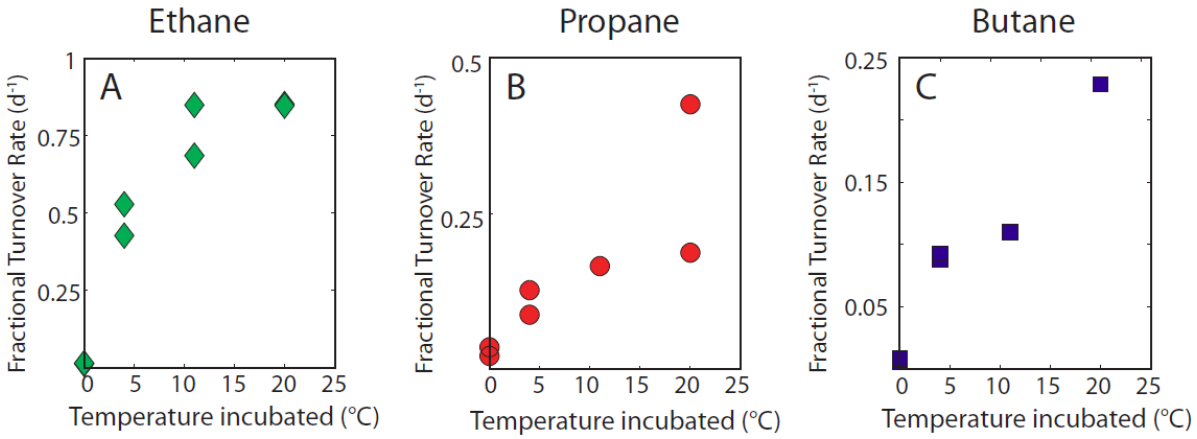

Figure 5. Temperature response experiment conducted as part of the method assessment for A) Ethane: Incubated with 2 µCi of tracer for 24h, B) Propane: Incubated with 2 µCi of tracer for 24h, and C) Butane: Incubated with 2 µCi of tracer for 24h. Duplicates are shown for each temperature.

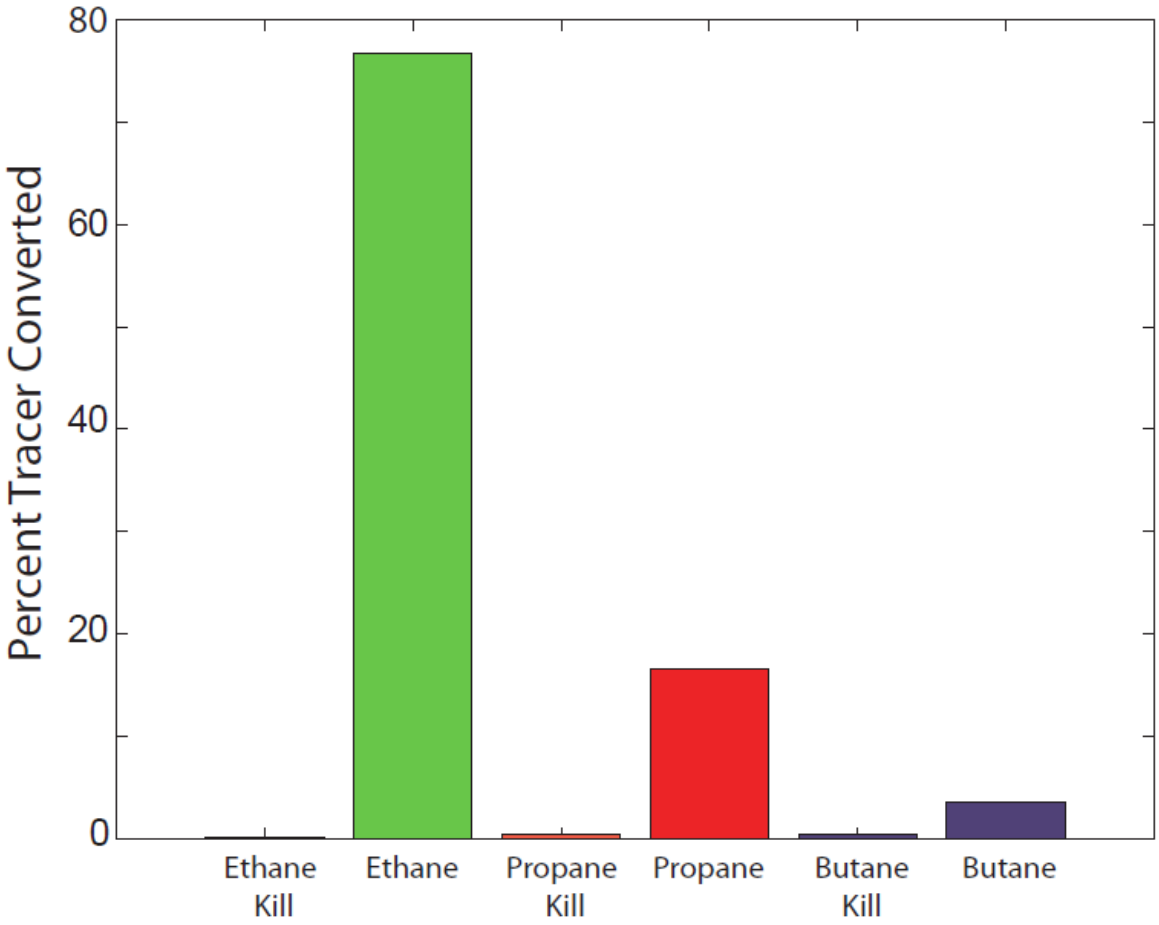

Figure 6. Comparison of tritiated ethane (green), propane (red), and butane (blue) converted during the kill control and rate incubation experiments collected for the method assessment (Table 1).

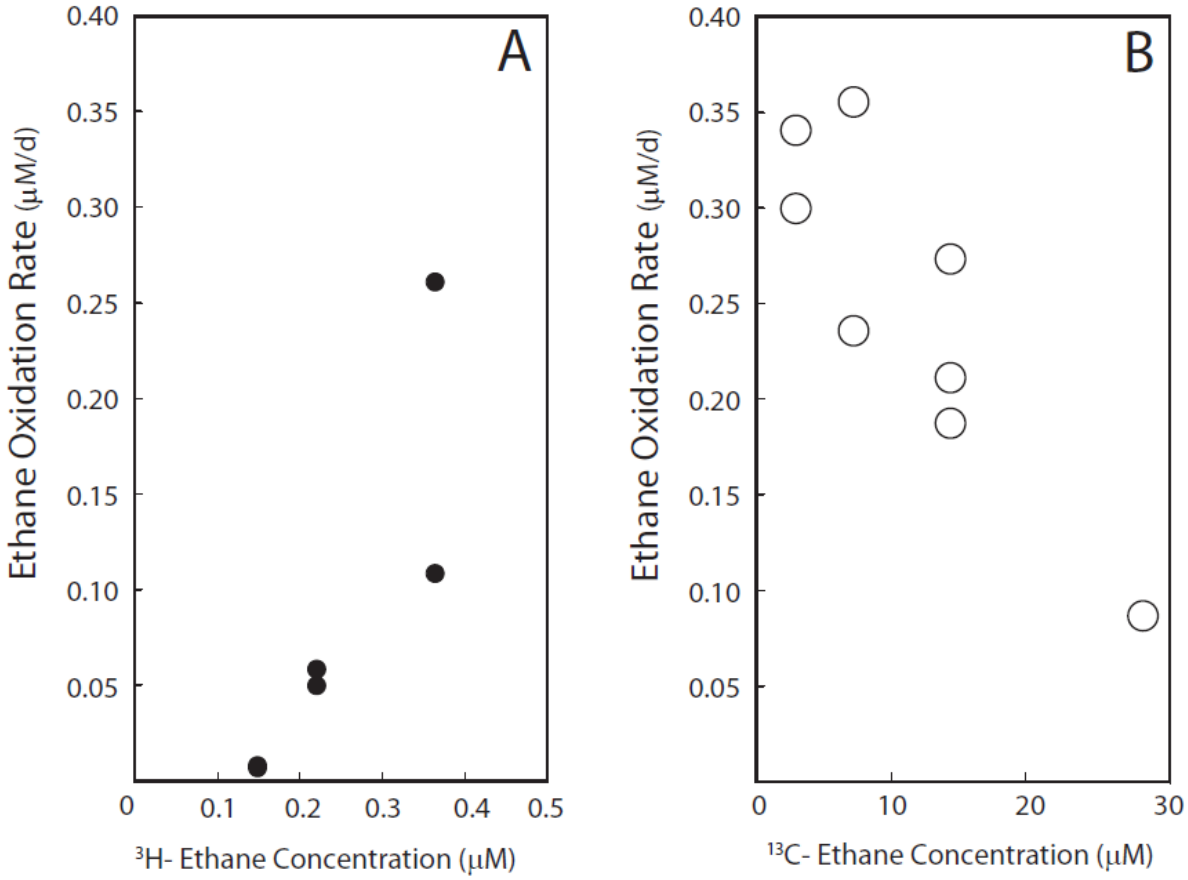

Figure 7. Ethane oxidation rates versus total concentration (ambient + tracer) in the bottle using (A) ^{3}H-ethane and (B) ^{13}C-ethane. Ambient ethane concentration was 77 nM. Note the different scales on the X-axes.

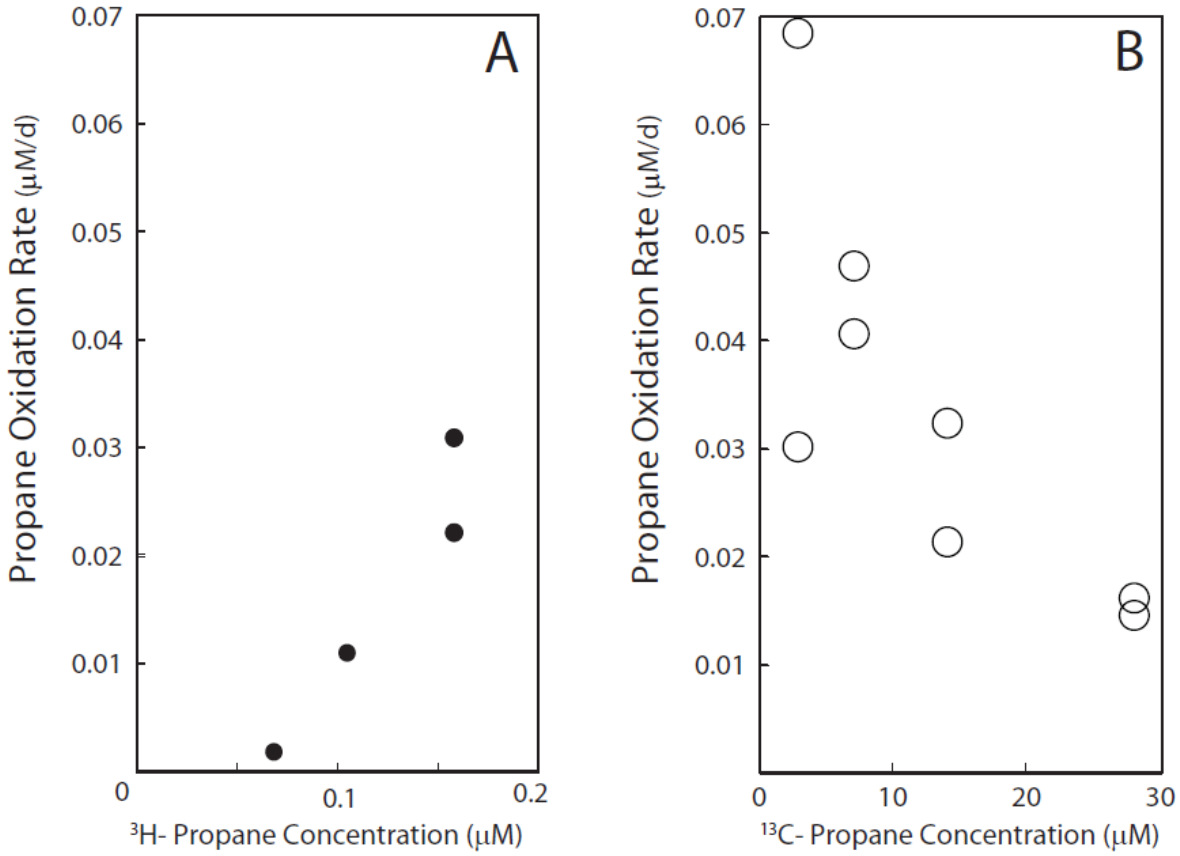

Figure 8. Propane oxidation rates measured versus total concentration (ambient + tracer) in the bottle using A) ^{3}H tracer and B) ^{13}C tracer. Ambient propane concentration was 51 nM. Note the different scales on the X-axes.

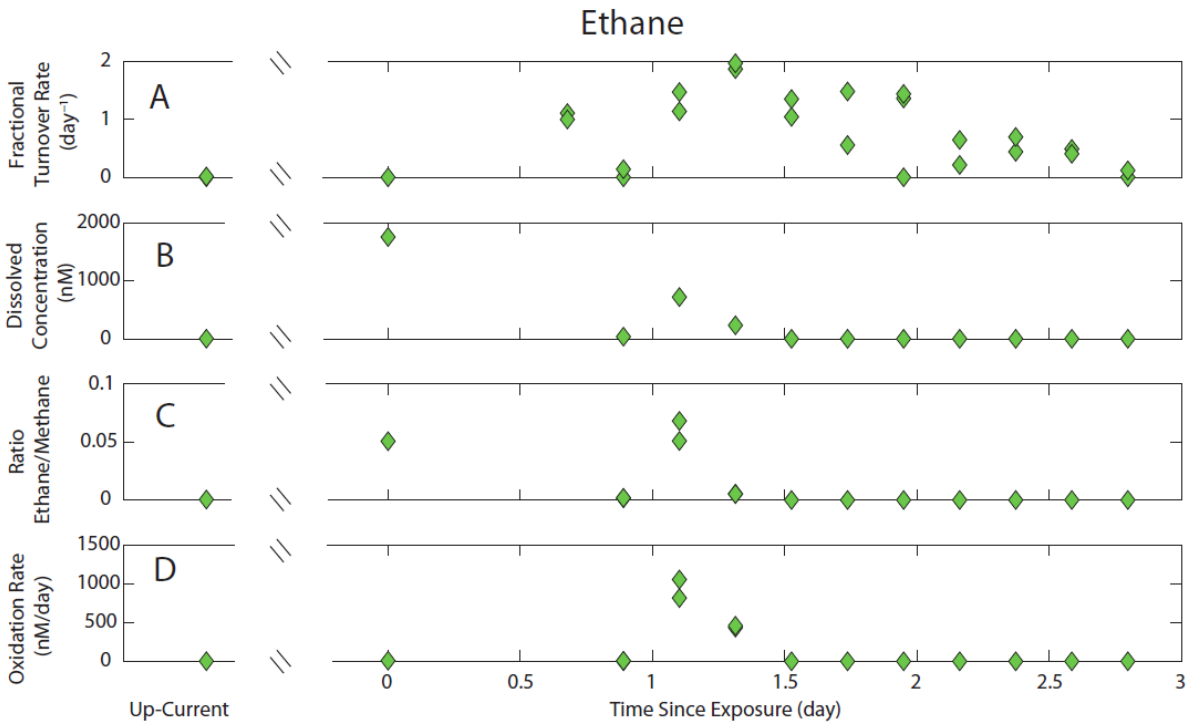

Figure 9. Ethane dynamics in the Coal Oil Point plume. A) Ethane fractional turnover rate (d^{-1}). B) Dissolved ethane concentration. C) The ratio of dissolved ethane to methane. D) Ethane oxidation rates. The x-axis represents the minimum time traveled from Coal Oil Point, assuming a linear trajectory. Coal Oil Point is located at 0 days.

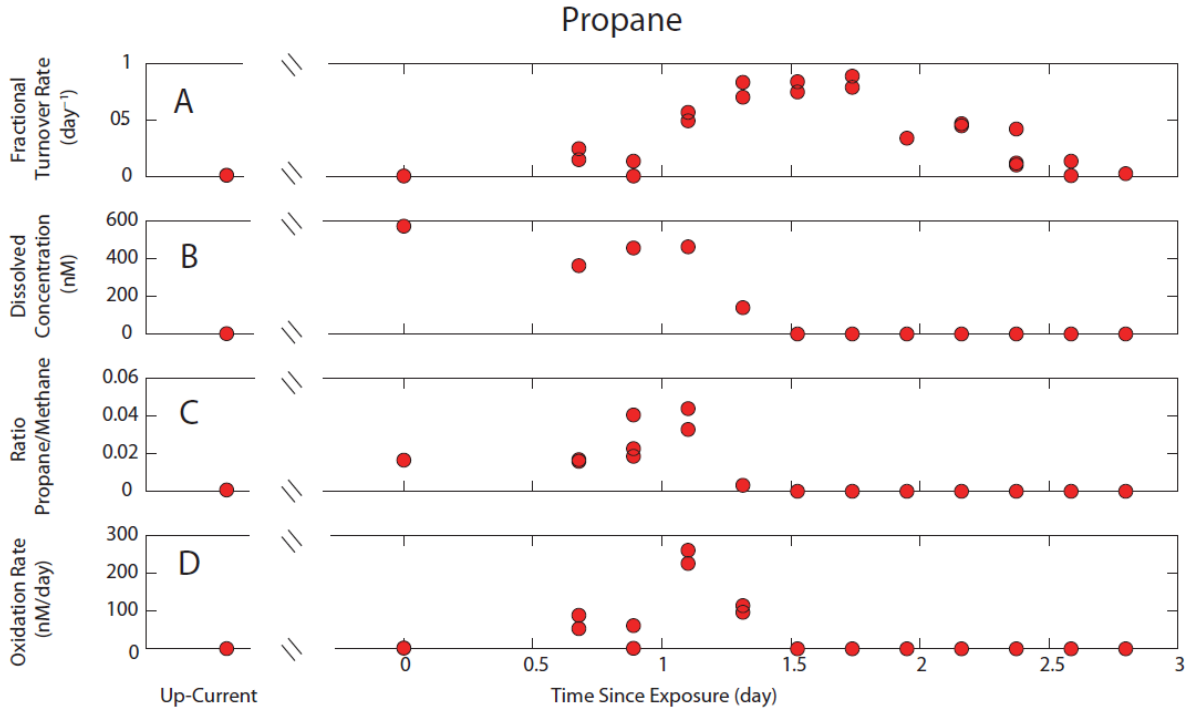

Figure 10. Propane dynamics in the Coal Oil Point plume. A) Propane fractional turnover rate (d^{-1}). B) Dissolved propane concentration. C) The ratio of dissolved propane to methane. D) Propane oxidation rates. The x-axis represents the minimum time traveled from Coal Oil Point, assuming a linear trajectory. Coal Oil Point is located at 0 days.

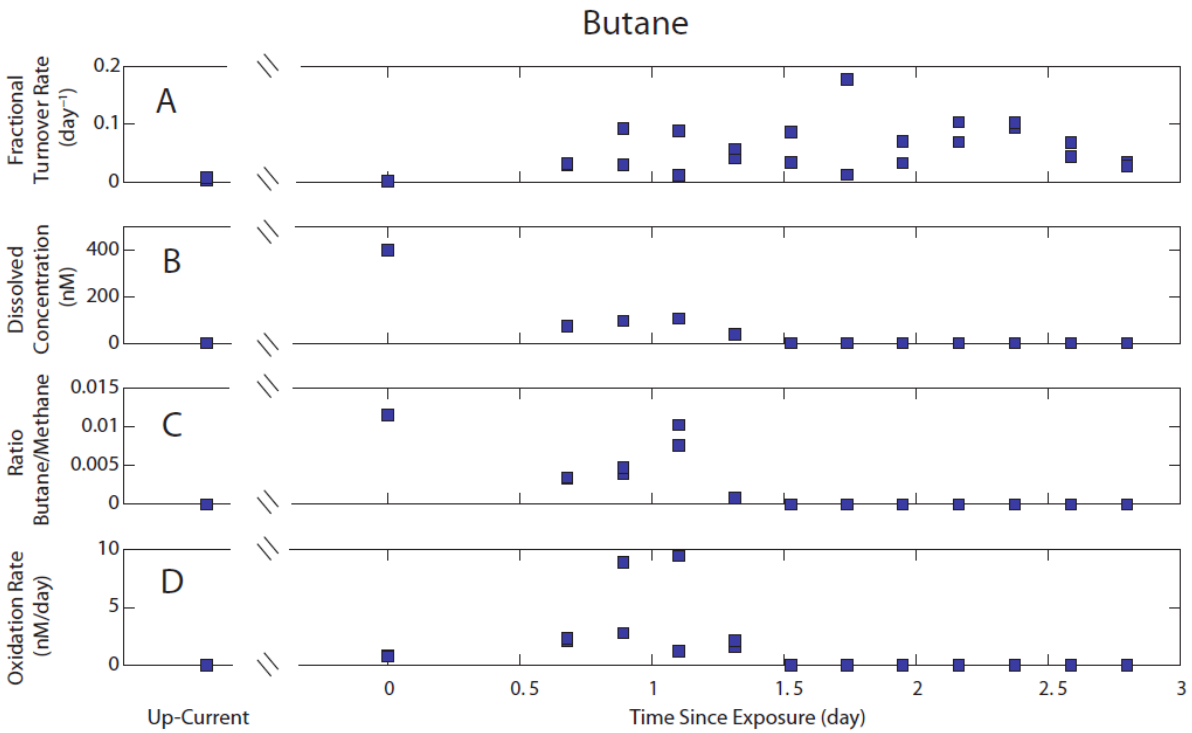

Figure 11. Butane dynamics in the Coal Oil Point plume. A) Butane fractional turnover rate (d^{-1}). B) Dissolved butane concentration. C) The ratio of dissolved butane to methane. D) Butane oxidation rates. The x-axis represents the minimum time traveled from Coal Oil Point, assuming a linear trajectory. Coal Oil Point is located at 0 days.

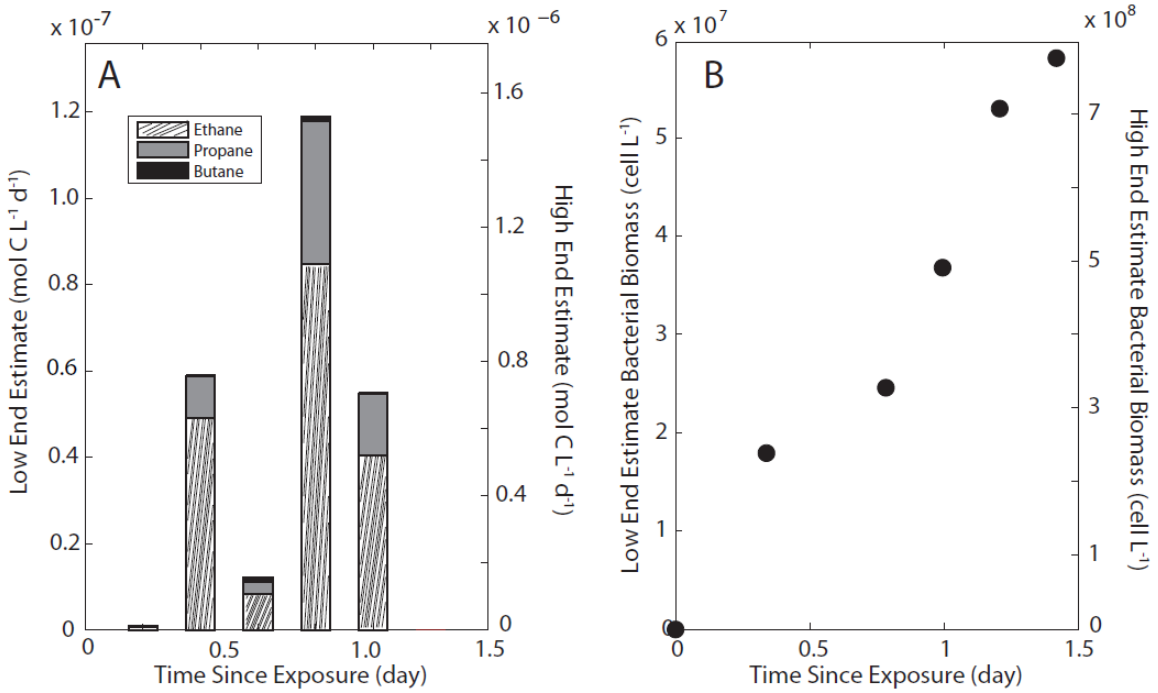

Figure 12. Estimates of microbial growth within the plume are calculated for A) Net bacterial production and B) Cumulative bacterial biomass from ethane, propane, and butane oxidizers. Growth efficiencies of 5% and 65% were used for the low-end and high-end estimates.

Table 1: Background chemical and physical conditions of the water mass collected for the method assessment experiment on September 21, 2011. The location is identical to station Plume 3 from Table 2.

Depth (m)	**Temp (°C)**	**Density (kg/m^3)**	**Salinity**	**O_2 (ml/l)**	**O_2 (%saturation)**	**[C_1H_4] (nM)**	**[C_2H_6] (nM)**	**[C_3H_8] (nM)**	**[C_4H_{10}] (nM)**
40	11.95	1025.45	33.29	4.44	72	2100	77	51	10

Table 2. Select properties of samples from the hydrocarbon plume.

Station	Depth (m)	Date Collected	Latitude	Longitude	Distance from COP (km)	[CH4] (nM)
Background	20	9/16/2011	34.358000°	-119.772000°	-8.1	66
COP	20-50	9/17/2011	34.375000°	-119.853167°	0	2000
Plume 1	25	7/31/2012	34.401650°	-119.929720°	8	1300
Plume 2	35	7/31/2012	34.411720°	-119.950870°	10.5	1250
Plume 3	54	7/31/2012	34.417666°	-119.983936°	13	720
Plume 4	45	8/2/2012	34.423830°	-120.011500°	15.5	2500
Plume 5	45	8/2/2012	34.434870°	-120.035070°	18	1500
Plume 6	45	8/2/2012	34.443980°	-120.055200°	20.5	1600
Plume 7	35	8/2/2012	34.444690°	-120.073580°	23	150
Plume 8	35	9/25/2012	34.444717°	-120.100967°	25.5	350
Plume 9	50	9/25/2012	34.445983°	-120.128283°	28	740
Plume 10	50	9/25/2012	34.451610°	-120.144270°	30.5	720

Table 3. Summary of the tracer synthesis. Percent yield was calculated with respect to water substrate. Specific Activity is reported in mCi per mmole of hydrocarbon.

Tritiated Tracer	Yield (%)	Specific Activity (mCi/mmol)
^{3}H-Ethane	36	77
^{3}H-Propane	57	400
^{3}H-Butane	37	420

Table 4. Incubation conditions for samples from the plume tracking.

Tracer (^{3}H)	**Activity (μCi)**	**Incubation Time (hours)**	**IncuationTemperature (°C)**
Ethane	2	12	11
Propane	1	24	11
Butane	2	24	11

IV. Anaerobic Oxidation of Ethane within Cold Seep Sediment from the Coal Oil Point Seep Field

Complete list of authors: Ryan Duncombe, Avi Rubin, Jeffery Shaffer, and David L. Valentine

Abstract

When short-chain hydrocarbons comprising natural gas – including methane and ethane – are released to the atmosphere they affect its chemistry and greenhouse warming. While many studies have considered the biological processes that prevent atmospheric release of methane from the ocean's floor, comparatively few have examined the metabolism of its analogs. Coal Oil Point, off the coast of Santa Barbara, CA, is the largest known natural marine hydrocarbon seep field in the world, with a persistent flux of thermogenically-derived natural gas that ranges from 1.4×10^9 to 4.8×10^9 g/yr for ethane. This study examined the metabolism of ethane in sediment collected from two individual seeps at this field: Campus Point Mounds and Patch seep. Ethane oxidation was quantified in slurry incubations under anaerobic conditions, demonstrating >97% ethane removal after 43 days when incubated near *in situ* temperature and ethane concentration. Ethane oxidation was also quantified in whole core profiles, which demonstrate elevated ethane oxidation rates to depths of 11 cm beneath sea floor, but rates below detection in the underlying zone of low sulfate. This study is the first to quantify anaerobic ethane oxidation within cold seep sediments. Total ethane consumption rates from Campus Point Mounds and Patch seep were calculated to be 2 μM day^{-1} and 0.012 μM day^{-1}, revealing anaerobic ethane oxidation in

sediment to be a dynamic process capable of modulating ethane's release into the ocean and atmosphere.

1. Introduction

Hydrocarbon seeps are an important source of natural gas, including methane (C1), ethane (C2), and propane (C3), into the ocean and atmosphere (Joye et al., 2004, Reeburgh 2007, Etiope et al., 2009). Marine seeps are globally distributed and can occur along both active and passive margins (Etiope et al., 2009, Kvenvolden and Rogers 2005, Skarke et al., 2014). Seeps form as gas and oil escape from underlying hydrocarbon reservoirs via faults and factures within Earth's crust, creating localized areas of emission at the seafloor. Sediments in and around areas of active seepage are characterized by elevated concentrations of simple (C1–C3) and complex (oils) hydrocarbons (Wilson et al., 1973, 1974). Substrate-rich sediment created by hydrocarbon seeps can host complex chemosynthetic microbial communities, facilitating both aerobic and anaerobic catabolism of the natural gas (Elvert and Niemann 2008, Kniemeyer et al., 2007, Valentine 2001).

The release of natural gases into the ocean and atmosphere is important due to their greenhouse potentials: C1, C2, and C3 have 21, 5.5, and 3.3 times the warming potential with respect to CO_2 (Singh et al., 1994, Jacob et al., 2002, Katzenstein et al., 2003). Methane is both the most abundant and best studied of the marine hydrocarbon gases (first paper on marine methane was published by Hutton and Zobell, 1949). Despite the presence of dissolved O_2 throughout most of the ocean's volume, consumption of methane is dominated by anaerobic processes within the sea floor (Reeburgh 2003) and accounts for a large sink in

the global methane budget (Reeburgh 2007, Valentine 2011). Anaerobic oxidation of methane is mediated by methanotrophic archaea associated with partners related to sulfate-reducing bacteria Holler et al., 2011), as initially identified in sediments overlying methane hydrates at Hydrate Ridge, Oregon (Boetius 2000). In marine sediments, rate measurements of sulfate reduction and methane oxidation suggest that most of the upward methane flux is oxidized anaerobically near the sulfate-methane interface (Reeburgh, 1976, Devol et al., 1984). Studies from Gulf of Mexico seep sites suggest that sulfate reduction is driven by both methane and non-methane hydrocarbons (Formolo et al., 2004).

Despite the importance of non-methane short-chain hydrocarbons, and the global abundance of these gases, relatively little is known about their anaerobic oxidation by marine microorganisms. Kniemeyer et al. (2007) reported the first quantitative measurements for anaerobic oxidation of propane and butane. Anaerobic oxidation of ethane was first reported in hydrothermal sediments of the Juan De Fuca Ridge by Adams et al. (2013); however, anaerobic oxidation of ethane within cold seeps has not been previously reported and is the focus of this study.

Anaerobic oxidation of ethane to CO_2 via sulfate reduction requires ethane and sulfate at a theoretical ratio of 4:7, as shown in Equation 1 below:

(EQ 1) $C_2H_6 + 1.75SO_4^{2-} \rightarrow 2HCO_3^- + 1.75HS^- + H_2O + 0.25H^+ + \{Biomass\}$

The location for this study is Coal Oil Point (COP), the world's largest and most characterized natural marine seep (Hornafius et al., 1999). Seepage from COP releases

petroleum otherwise trapped in the Miocene-aged Monterey Formation (Ogle et al. 1987). Total gas flux from the seep field was calculated to be 5.9 to 19.3 x 10^4 m^3 day^{-1} from sonar estimates, with a natural gas composition of 87.5% C1, 5.1% C2, and 3.1% C3 (Clark et al. 2000). Ethane emission rates into the water column range from 1.3 to 4.4×10^5 mol day^{-1}, with roughly equal amounts dissolving into the water column and being released directly into the atmosphere (Clark et al. 2000, Leifer and Clark 2001).

This biogeochemical investigation aimed to assess: 1) the native capacity for anaerobic oxidation of ethane in marine sediments from a hydrocarbon seep, and 2) the depth distribution of ethane oxidation rates in contrasting hydrocarbon seeps. These aims were achieved by tracking ethane consumption in sediment slurries and intact cores, using both a tritiated tracer approach as well as other supportive chemical measurements.

2. Method

2.1 Study Sites

Sediment samples were collected from two locations within the COP seep field: Patch seep (water depth 70 m) and Campus Point Mounds (CPM, water depth 48 m) (Table 1), during an expedition with the *RV Atlantis* and *ROV Jason* on October 6, 2013 (Figure 1). Patch seep and CPM combine to cover over 4000 m^2 of the sea floor in the Santa Barbara Channel. Sediment samples were collected via *ROV Jason* (dives: J2-739 and J2-740) by push coring (6.3 cm in diameter) and processed shipboard.

2.2 Preparation of Slurry Incubations

Slurry incubations were analyzed for both dissolved hydrocarbon concentration (section 2.7.2) and ethane oxidation rates (section 2.8.2). Sediment slurry vials were prepared and assembled in an anoxic glove box. Sediment was mixed with anoxic seawater at a ratio of 2:1 water to sediment, poured into 60 mL serum bottles, sealed with gas tight chlorobutyl rubber stoppers, crimped, and then incubated at 11°C. Sediment cores were divided into upper and lower sections based on sulfate profiles. Sediment above the sulfate to sulfide transition zone was considered upper (<8 cm); sediment within the zone of decreasing sulfate and increasing sulfide was considered lower (>8 cm). Upper and lower sections were each homogenized in a container of sterile seawater containing degassed 1 mM Na_2S (to ensure anoxic conditions). Slurry mixtures were degassed by bubbling with N_2 for 1.5 hours in a glove box to remove dissolved hydrocarbon within the sediment and then transferred into 60 mL serum bottles. Seawater used to make the slurry was collected from COP, sterilized through a 0.2 µm filter, and degassed using N_2 for a minimum of 1 hour. Filtered seawater was chosen over artificial seawater to reduce the possibility of nutrient or sulfate limitation. After bottles were completely filled with the slurry mixture (no headspace), 50 µM of ethane was added to each bottle via a syringe. A total of 18 replicate bottles were prepared for each set (upper and lower core) of non-kill experiments. Replicate bottles were harvested in groups of three for each sampling event. For kill control experiments, replicate bottles were harvested in pairs, at every other sampling event. To establish kill control bottles, 0.25 mL of saturated mercuric chloride solution was added prior to the ethane.

2.3 Sediment Porewater Extraction

Push cores used for porewater extraction were equipped with two sets of predrilled holes at 2 cm resolution and sealed with electrical tape prior to deployment. Fluid was extracted horizontally as similarly described in Seeberg-Elverfeldt et al. (2005), using rhizons attached to a flushed syringe under vacuum. Extracted porewater was immediately analyzed for sulfate and sulfide concentration or subsampled and stored for $\delta^{13}C$ of dissolved inorganic carbon.

2.4 Dissolved Sulfate and Sulfide Concentrations

Sulfate measurements were calibrated against the International Association for the Physical Sciences of the Ocean (IAPSO) standardized seawater (28.9 mM SO_4^{2-}). For each measurement, 200 µL of extracted porewater was added to 4 mL of deionized water then treated with excess $BaCl_2$ (Gieskes, 1991) and measured on an UV-Vis spectrophotometer set at 400 nm; the calibration curve was deemed to be acceptable if $R^2 > 0.96$. The error associated with this method was ±0.05 mM. Sulfide measurements were taken on a UV-Vis spectrophotometer set at 480 nm using a mixture of 100 µL of sample and 4 mL of 5 mM $CuSO_4$ (Cord-Ruwisch et al. 1985); calibration curves was deemed to be acceptable if $R^2 > 0.99$. The error associated with this method was ±1.9 mM.

2.5 $\delta^{13}C$- DIC

The ^{13}C of dissolved inorganic carbon (DIC) in porewater was determined using methods described in Chapter 3 (method section 2.2.5). Samples were prepared by

acidifying 1.0 mL of sample with 0.5 mL of 85% H_3PO_4. The sample was allowed to equilibrate overnight and the resulting CO_2 was injected into an isotope ratio mass spectrometer (IRMS) coupled with a Finnigan Gas Bench. Ten aliquots of the sample were delivered to the IRMS via a sample loop and analyzed along with four aliquots of house CO_2 gas, three before and one after the sample aliquots. ^{13}C values were calculated with reference to the laboratory house CO_2 gas. Data were normalized using LSVEC Li_2CO_3 isotope reference material, which resulted in a standard deviation of 0.17.

2.6 Porewater Fraction in Sediment

The fraction of sediment occupied by pore fluid was determined by drying a known volume and weight of wet sediment. Samples were dried at 60°C over 48 hours and reweighed. Porewater fraction was calculated by dividing the difference between the two weights by the wet weight.

2.7 Hydrocarbon Concentration Measurements

2.7.1 Whole Core Profiles

Sediment was extruded from the core liner in 2 cm sections. Sediment was immediately placed into degassed 40 mL serum vials containing 10 mL of 2 M NaOH, using a 3 mL cut-off syringe. Dissolved hydrocarbon gases from the sediment equilibrated with the vial's headspace for a minimum of 24 hours before analysis. Headspace concentrations of methane, ethane, and propane were quantified using a Shimadzu GC 14A gas chromatograph equipped with a flame ionization detector (GC-FID), with an associated

error of ±0.02 µM. Analytes were resolved at isothermal 60°C conditions using N_2 as the carrier gas through a 12’ x 1/8” packed column (n-octane on Res-Sil C) (Quistad et al. 2010).

2.7.2 Slurry

Dissolved gas concentrations were analyzed using similar methods as described in section 2.7.1. Using a 20 mL syringe equipped with a stopcock, 5 mL of water was removed from the slurry vials, and replaced with 5 mL degassed artificial seawater. The 20 mL syringe was supplemented with a headspace of 10 mL of N_2 gas, shaken vigorously, and allowed to equilibrate for 12-24 hours. Following headspace equilibration, 3 mL samples of headspace gas were injected into a GC-FID to determine the concentrations of ethane.

2.8 Quantifying Ethane Oxidation Rates

Tritium-labeled tracers were used to quantify the rate of ethane consumption for each incubation. Tritiated tracers were previously used by Reeburgh et al. (1991) to measure methane oxidation rates in marine environments. Tritiated ethane used in this study was synthesized using the methods described in chapter 3, section 2.1.

2.8.1 Vertical Distribution of Ethane Oxidation Rates in Intact Cores

Tritium-labelled ethane tracer was prepared by dissolving the stock tritiated ethane into degassed artificial seawater (35 g/L NaCl). This solution was injected at 1 cm intervals (0.41 µCi of tracer per cm) along the length of each core. Cores were then incubated for 24

hours at *in situ* temperature. Following incubation, 1 mL of the sediment/liquid mixture at each interval was measured on a liquid scintillation counter (LSC). The kill control cores were sterilized using a bench top autoclave (110°C at 20 psi for 1.5 hours) to kill active microbes present in the sediment. These cores were then incubated in parallel to the live cores to quantify the background rate of non-biological isotope exchange.

2.8.2 Slurry Sediment Oxidation Rates

Slurry samples were prepared in an anoxic glove box and treated with 50µM of ethane. A total of 18 replicate bottles were prepared for each set (upper and lower core) of non-kill experiments. Replicate bottles were harvested in groups of three for each sampling event. Time series measurements were conducted over a period of 70 days using sacrificial sampling. At the chosen times, vials were selected in triplicate, injected with 0.5 µCi of tritiated ethane and incubated for 24 hours. Vials were subsequently injected with a solution of saturated mercuric chloride and bubbled with N_2 in a fume hood to halt biological activity and remove any unreacted substrate. An aliquout of the slurry was analyzed by the LSC to determine the amount of product produced during the incubations. Oxidation rates were calculated using the equations outlined in section 2.8.3. Kill controls were handled in a manner similar to non-kill samples, except that they were sampled in duplicate.

2.8.3 Calculations

Oxidation rates for ethane were quantified in the whole core and slurry incubations using equations 2-3. The fractional turnover rate, FTR, represents the fraction of tracer

consumed during incubation where A_p represents the amount of activity produced after incubation, A_k is the activity with the kill controls and accounts for any abiotic tracer conversion, A_i represents the amount of tritiated ethane injected, and I_t is the total incubation time (equation 2):

(EQ 2) $FTR = [(A_p - A_k)/(A_i)]/(I_t)$

The rate of ethane oxidation is converted to an *in situ* value by multiplying the pseudo-first order rate constant (FTR) with the ambient ethane concentration, [C2] (equation 3). Units for oxidation rate are in μM $days^{-1}$, which represents the rate of ethane consumption for a given locality.

(EQ 3) $Ox = FTR * [C2]$

3. Results

3.1 Sediment Slurry

Sediment cores collected from both Patch seep and CPM were divided into two sections, upper (0-8 cm) and lower (8-16 cm), and incubated under sulfidic conditions with 50 μM of ethane, for a duration of two months. Time series incubation results are presented in figure 2 (Campus Point Mounds) and figure 3 (Patch seep). Experimental detection limits, equivalent to background FTR signals, were calculated by adding the average oxidation rate

from kill control data to the 2σ error. For CPM and Patch seep, detection limits were 0.002 day^{-1} and 0.003 day^{-1}, respectively.

Ethane was found to be consumed anaerobically in all treatments and at both locations. For CPM samples, >97% of the ethane was consumed for each of the 18 samples harvested after 43 days of incubation (figure 2A). For Patch Seep, 10 of 12 samples displayed ethane consumption exceeding 93% when harvested after more than 43 days (figure 3A). However, the rate of ethane loss was not linear: 15 of 18 samples harvested in the first 19 days of the incubation had consumed <6% of available ethane. The acceleration in ethane consumption rate is indicative of microbial growth and adaptation more so than *in situ* activity. Ethane remained at relatively low concentrations from day 43 until the incubations concluded at day 70 for both upper and lower samples from each location. Averaging those measurements, ethane concentrations reached a minimum threshold of 1.3 ± 0.8 μM.

The measurement of ethane oxidation rates using tritium-labelled ethane also yielded evidence for oxidation, consistent in pattern with the concentration measurements. At CPM, fractional turnover rates reached an observed maximum of 0.05 day^{-1} for the upper and 0.04 day^{-1} for the lower core slurries (at day 43 of the incubation); at Patch seep, rates reached a maximum of 0.04 day^{-1} for upper core slurries and 0.10 day^{-1} for lower core slurries (also at day 43 of the incubation). The pattern observed for all samples and at both locations was similar: low and consistent oxidation rates gave way to elevated but variable rates as substrate was depleted. Peak rates of oxidation likely occurred between 20 and 43 days of incubation, but were not effectively captured by the chosen sampling intervals.

3.2 Sediment Depth Profiles

3.2.1 Campus Point Mounds

Depth profiles of sediment chemistry and microbial activity of CPM samples are presented in figure 4. Hydrocarbon concentrations (C1-C3) were generally lower at the surface and higher with depth (to a total depth of 22 cm), with a short deviation from this trend between 10 to 15 cm. Shallowest samples (0-2 cm) contained 170 µM, 4 µM, and 1.4 µM for methane, ethane, and propane, respectively, whereas deepest samples (20-22 cm) contained 900 µM, 250 µM, 130 µM.

Ethane fractional turnover rates also increased with depth, reaching a maximum rate of 0.008 day^{-1} (figure 4) between 7 and 9 cm. Rates began to drop by 9 cm and fell below detection limit by 12 cm. Experimental detection limits were calculated by adding the average oxidation rate from kill control data to the 2σ error. For CPM the background FTR was 0.001 day^{-1}, as determined by this method. Sulfate concentrations mirrored trends observed in the fractional turnover rates (the highest ethane fractional turnover rates occurred in regions of high sulfate concentration). At depths of 0-10 cm, sulfate concentrations were relatively high, ranging from 15 to 28 mM. Below 10 cm, sulfate concentrations dropped to a low of 5 mM. Sulfide concentrations had the opposite trend: low (0-1 mM) in shallow sediment, but increased slightly (2-4 mM) below 10 cm.

3.2.2 Patch Seep

Depth profiles of sediment chemistry and microbial activity of Patch seep samples are presented in figure 5. As was observed in the CPM seep samples, dissolved hydrocarbon

concentrations for C1-C3 were generally lower at the surface and higher with depth. However, concentrations at Patch seep reached a maximum at 12 cm before decreasing slightly with depth. The upper 12 cm of the sediment averaged 300 µM, 410 µM, and 94 µM for methane, ethane, and propane, respectively; samples at 12 cm (highest concentrations) were 1200 µM, 1400 µM, 390 µM.

Ethane fractional turnover rate increased with depth and reached a maximum of 0.005 day^{-1} at 5 cm below sea floor (figure 5). Fractional turnover rates fell below detection limit at depths >10 cm. Experimental detection limits were calculated as described above and for Patch seep the background FTR was 0.002 day^{-1}. Sulfate concentrations again were predictive of fractional turnover rates. At depth <6 cm sulfate concentrations were high, ranging from 18-22 mM, while at depth >6 cm, concentrations were <10 mM. Sulfide concentrations were low (0-1 mM) in upper sediments, but increased to 5mM at 10 cm.

4. Discussion

4.1 Anaerobic Oxidation of Ethane in Slurry Incubations

Slurry incubations of both upper and lower intervals from CPM and Patch seep sediments show similar trends in the consumption pattern: ethane concentrations decreased as oxidation rate increased. Ethane concentrations in the slurry experiments decreased until reaching a threshold value of 1.3 ± 0.8 µM (median value 0.9 µM). Fractional turnover rates increased with time and were sustained above initial rates even after substrate was effectively, but not completely, consumed (figures 2, 3). This suggests that ethane must be present above this minimum threshold for appreciable oxidation to occur under anaerobic

conditions, effectively identifying a threshold concentration for the anaerobic oxidation of ethane that is similar if not slightly lower than that observed for methane (Valentine, 2011).

Fractional turnover rates for a 24 hour incubation were 0.01 day^{-1} for CPM and Patch seep, with anaerobic oxidation of ethane evident from the onset of the experiment (figure 2B, 3B). Initial oxidation rates, normalized to the volume of added porewater, were 20 µM day^{-1} and 13 µM day^{-1} for lower and upper sections of CPM core intervals, respectively. Initial oxidation rates, normalized to porewater volume, were 21 µM day^{-1} and 11 µM day^{-1} for lower and upper sediment intervals from Patch Seep, respectively. Oxidation rates determined in the slurry experiments are not a direct proxy for *in situ* consumption rates due to the inherent differences in methods. However, the immediate capacity of the sediments to consume ethane suggests *in situ* activity for both depth intervals. The observation that the lower intervals yielded higher rates of oxidation than the upper intervals stands in contrast to the results observed from the whole-core approach and may relate to improved substrate availability for the slurry incubations. The observation of long-term consumption is consistent with a recent report from hydrothermal systems at Middle Valley, Juan de Fuca Ridge (Adams et al., 2013).

4.2 Ethane Oxidation within Intact Sediment Cores

Rate measurements of ethane oxidation were conducted on whole core sediment profiles from two seeps within the COP seep field. Ethane oxidation rates from both CPM and Patch seeps were highest in shallow sediments, which contained >20 mM sulfate and <2 mM sulfide (Figure 4, 5). High sulfate/low sulfide concentrations leave open the possibility

for the presence of alternate electron acceptors (e.g., oxygen, manganese, nitrate, or iron) (Jørgensen and Nelson 2004). The transition to low sulfate concentrations occurred below about 8 cm at both seep sites, consistent with sulfate utilization for anaerobic oxidation of ethane at depths >8 cm. However, the data for the upper sediment section is equivocal on this point.

Fractional turnover rates were elevated in upper sections of intact sediments cores at both seep locations. Elevated rates in the surface sediment could be related to the presence of alternative electron acceptors not present in lower sediment, such as oxygen (Redmond et al. 2010, Kinnaman et al. 2007). Dissolved oxygen advects into seep sediments from the overlying water column and the possibility for aerobic metabolism cannot be excluded for the experiments using intact cores. However, the presence of abundant sulfide and the immediate activity observed in the slurry experiments indicate that the capacity for anaerobic oxidation of ethane is present in this sediment interval.

4.3 Ethane Oxidation Potential

Estimates of total ethane consumption were scaled for each seep and for each experiment to gauge the importance of this process as a sink of ethane. From the slurry incubations we calculate a potential rate from the initial oxidation rate, normalized by pore fluid volume and scaled to the volume of the seep (assuming a uniform depth of 16 cm). CPM seepage covers a total area of about 1000 m^2 and Patch covers about 3000 m^2 (Table 1). The resulting values of 410 mmol day^{-1} and 1000 mmol day^{-1} provide one estimate for ethane consumption for CPM and Patch, respectively.

From the whole core incubations we estimated rates by summing the depth integrated consumption rate and extrapolating out to the size of the seep. Depth integrated rates were calculated by summing the total ethane oxidation rate of each core. Depth normalized ethane oxidation rates for CPM and Patch seeps are 2 μM day^{-1} and 0.012 μM day^{-1}, respectively. Whole core oxidation rate measurements were conducted from sediment cores of 1 cm diameter; therefore, the cumulative ethane oxidation rate for the sediment column represents a footprint of $8x10^{-5}$ m^2. These rates are then extrapolated out to the size of the seep. The rate of total ethane oxidation from CPM and Patch seep is 3200 mmol day^{-1} and 18 mmol day^{-1}, respectively.

We view these estimate as theoretical maximums even though the two approaches produced a wide range of values. Seep environments, even within one sediment core, are not uniform in ethane concentration, porosity, or in oxidation rates. Small variations propagate through the calculation. These two approaches resulted in a range of 410 mmol day^{-1} and 3200 mmol day^{-1} for CPM and a range of 18 mmol day^{-1} to 1000 mmol day^{-1} for Patch seep ethane consumption. Ultimately, the microbial oxidation of ethane is an important biofilter that regulates the total amount of gas released from seep environments, and additional measurements are needed to better define its variability and efficacy.

5. Conclusions

Ethane oxidation is active in the upper 8-10 cm of cold seep sediment cores. High fractional turnover rates corresponded with zones of high sulfate concentrations (>10mM). Oxidation rates and sulfate concentrations decreased in deeper sediment, suggesting that

anaerobic ethane oxidation was at or below detection limits in the whole core profiles (1 day incubation time; CPM 0.001 day^{-1}, Patch 0.002 day^{-1}). Conversely, anoxic slurry experiments, with longer incubation times, showed a clear increase in microbial activity within 40 days. Ethane was effectively, but not completely, removed from in slurry vials by day 43. For oxidation to occur, ethane concentration had to exceed the minimum threshold of 1.3 μM ± 0.8. This study is the first to observe anaerobic oxidation of ethane in cold seep sediments. Extrapolations based on the different methods suggest that a total of 410 mmol day^{-1} to 3200 mmol day^{-1} and 18 mmol day^{-1} to 1000 mmol day^{-1} of ethane are consumed at CPM and Patch seep, respectively.

References:

Adams, M. M., A. L. Hoarfrost, S. Bose, S. B. Joye, P. R. Girguis (2013). Anaerobic oxidation of short-chain alkanes in hydrothermal sediments: potential influences on sulfur cycling and microbial diversity, *Frontiers in Microbiology*, 4. doi:10.3389/fmicb.2013.00110

Arp, D. J. (1999). Butane metabolism by butane-grown 'Pseudomonas butanovora', *Microbiology*, 145(5), 1173-1180.

Ashraf, W., A. Mihdhir, and C.J. Murrell (1994). Bacterial oxidation of propane. FEMS Microbiology Letters, 122(1), 1-6.

Boetius, A., Ravenschlag, K., Schubert, C. J., Rickert, D., Widdel, F., Gieseke, A., Amann, R., Jørgensen, B., Witte, U., and Pfannkuche, O. (2000). A marine microbial consortium apparently mediating anaerobic oxidation of methane. *Nature*, 407(6804), 623-626.

Clark, J. F., Washburn, L., Hornafius, J. S., & Luyendyk, B. P. (2000). Dissolved hydrocarbon flux from natural marine seeps to the southern California Bight. *Journal of Geophysical Research: Oceans* (1978–2012), 105(C5), 11509-11522.

Clark, J. F., L. Washburn & K. S. Emery (2010). Variability of gas composition and flux intensity in natural marine hydrocarbon seeps (vol 30, 379, 2010). *Geo-Marine Letters*, 30, 389-389.

Cord-Ruwisch, R. (1985). A quick method for the determination of dissolved and precipitated sulfides in cultures of sulfate-reducing bacteria. *Journal of Microbiological Methods*, 4(1), 33-36.

Dartnell, P., E. Phillips, D. Finlayson, J. Conrad, and R. Kvitek (2014). Colored shaded-relief bathymetry, Offshore of Coal Oil Point map area, California, sheet 1 in Johnson, S.Y., P. Dartnell, G. Cochrane, n. Golden, E. Phillips, A. Ritchie, R. Kvitek, B. Dieter, J. Conrad, T. Lorenson, L. Krigsman, H. Greene, C. Endris, G. Seitz, D. Finlayson, R. Sliter, F. Wong, M. Erdey, C. Gutierrez, I. Leifer, M. Yoklavich, A. Draut, P. Hart, F. Hostettler, K. Peters, K. Kvenvolden, R. Rosenbauer, and G. Fong, (S.Y. Johnson and S.A. Cochran, eds.), California State Waters Map Series— Offshore of Coal Oil Point, California: U.S. Geological Survey Scientific Investigations Map 3302, pamphlet 57 p., 12 sheets, scale 1:24,000, http://dx.doi.org/10.3133/sim3302.

Elvert, M., & Niemann, H. (2008). Occurrence of unusual steroids and hopanoids derived from aerobic methanotrophs at an active marine mud volcano. *Organic Geochemistry*, 39(2), 167-177.

Etiope, G. & P. Ciccioli (2009). Earth's degassing: A missing ethane and propane Source. *Science*, 323, 478-478.

Etiope, G., K. R. Lassey, R. W. Klusman & E. Boschi (2008). Reappraisal of the fossil methane budget and related emission from geologic sources. *Geophysical Research Letters*, 35, 5.

Formolo, M. J., Lyons, T. W., Zhang, C., Kelley, C., Sassen, R., Horita, J., & Cole, D. R. (2004). Quantifying carbon sources in the formation of authigenic carbonates at gas hydrate sites in the Gulf of Mexico. *Chemical Geology*, 205(3), 253-264.

Gieskes, J. M., Gamo, T., & Brumsack, H. (1991). Chemical methods for interstitial water analysis aboard JOIDES Resolution. *Ocean Drilling Program*, Texas A & M University.

Hornafius, J.S., D.C. Quigley, and B.P. Luyendyk (1999). The world's most spectacular marine hydrocarbon seeps (Coal Oil Point, Santa Barbara Channel, California): Quantification of emission, J. *Geophysical Research Letters*, 104(C9), 20,703– 20,711.

Hutton, W. E., & ZoBell, C. E. (1949). The occurrence and characteristics of methane-oxidizing bacteria in marine sediments. *Journal of bacteriology*, 58(4), 463.

Jacob, D. J., B. D. Field, E. M. Jin, I. Bey, Q. B. Li, J. A. Logan, R. M. Yantosca & H. B. Singh (2002). Atmospheric budget of acetone. *Journal of Geophysical Research-Atmospheres*, 107.

Jørgensen, B. B., & D.C. Nelson (2004). Sulfide oxidation in marine sediments: geochemistry meets microbiology. *Geological Society of America Special Papers*, 379, 63-81.

Joye, S. B., Boetius, A., Orcutt, B. N., Montoya, J. P., Schulz, H. N., Erickson, M. J., & Lugo, S. K. (2004). The anaerobic oxidation of methane and sulfate reduction in sediments from Gulf of Mexico cold seeps. *Chemical Geology*, 205(3), 219-238.

Katzenstein, A. S., L. A. Doezema, I. J. Simpson, D. R. Balke & F. S. Rowland (2003). Extensive regional atmospheric hydrocarbon pollution in the southwestern United States. Proceedings of the National Academy of Sciences of the United States of America, 100, 11975-11979.

Kinnaman, F. S., D. L. Valentine & S. C. Tyler (2007). Carbon and hydrogen isotope fractionation associated with the aerobic microbial oxidation of methane, ethane, propane and butane. *Geochimica Et Cosmochimica Acta*, 71, 271-283.

Kniemeyer, O., F. Musat, S. M. Sievert, K. Knittel, H. Wilkes, M. Blumenberg, W. Michaelis, A. Classen, C. Bolm, S. B. Joye & F. Widdel (2007). Anaerobic oxidation of short-chain hydrocarbons by marine sulphate-reducing bacteria. Nature, 449, 898-U10.

Kvenvolden, K. A., & Rogers, B. W. (2005). Gaia's breath—global methane exhalations. Marine and *Petroleum Geology*, 22(4), 579-590.

Leifer I, Clark J (2001). Modeling trace gases in hydrocarbon seep bubbles. Application to marine hydrocarbon seeps in the Santa Barbara Channel. *Russ Geol Geophys* 43:613–621

Mau S, Valentine DL, Clark JF, Reed J, Camilli R, Washburn L (2007). Dissolved methane distributions and air-sea flux in the plume of a massive seep field, Coal Oil Point, California. Geophys Res Lett 34:L22603. doi:10.1029/2007GL031344

Nielsen LP, Risgaard-Petersen N, Fossing H, Christensen PB, Sayama M. (2010). Electric currents couple
spatially separated biogeochemical processes in marine sediment. *Nature* 463:1071–74

Perry, J. J. (1979). Microbial cooxidations involving hydrocarbons. *Microbiological Reviews*, 43(1), 59.

Ogle, B. A., Wallis, W. S., Heck, R. G., & Edwards, E. B. (1987). Petroleum geology of the Monterey Formation in the offshore Santa Maria/Santa Barbara areas. Cenozoic basin development of coastal California, Rubey, 6, 382-406.

Quistad, S.D., and D.L. Valentine (2011). Anaerobic propane oxidation in marine hydrocarbon seep sediments, *Geochim Cosmochim Acta*, 75(8), 2159-2169.

Redmond, M.C., and D.L. Valentine (2012). Natural gas and temperature structured a microbial community response to the Deepwater Horizon oil spill, *Proceedings of the National Academy of Sciences*, 109(50), 20292-20297. doi:10.1073/pnas.1108756108

Redmond, M.C., D.L. Valentine, and A.L. Sessions (2010). Identification of novel methane-, ethane-, and propane-oxidizing bacteria at marine hydrocarbon seeps by stable isotope probing. Applied and Environmental Microbiology, 76(19), 6412-6422.

Reeburgh, W. S. (1976). Methane consumption in Cariaco Trench waters and sediments. *Earth and Planetary Science Letters*, 28(3), 337-344.

Reeburgh, W. S. (2003). Global methane biogeochemistry. *Treatise on geochemistry*, 4, 65-89.

Reeburgh, W.S. (2007). Oceanic methane biogeochemistry, *Chemical Reviews*, 107, 486–513.

Seeberg-Elverfeldt, J., Schlüter, M., Feseker, T., & Kölling, M. (2005). Rhizon sampling of pore waters near the sediment/water interface of aquatic systems. *Limnology and oceanography: Methods*, 3, 361-371.

Skarke , A., C. Ruppel, M. Kodis, D. Brothers, and E. Lobecker (2014). Widespread methane leakage from the sea floor on the northern US Atlantic margin. *Nature Geosciences*.

Singh, H. B., D. Ohara, D. Herlth, W. Sachse, D. R. Blake, J. D. Bradshaw, M. Kanakidou & P. J. Crutzen (1994). Acetone in the atmosphere - Distributions, Sources, and Sinks. *Journal of Geophysical Research-Atmospheres*, 99, 1805-1819.

Treude, T., A. Boetius, K. Knittel, K. Wallmann & B. B. Jorgensen (2003). Anaerobic oxidation of methane above gas hydrates at Hydrate Ridge, NE Pacific Ocean. *Marine Ecology-Progress Series*, 264, 1-14.

Treude, T., & Ziebis, W. (2010). Methane oxidation in permeable sediments at hydrocarbon seeps in the Santa Barbara Channel, California. *Biogeosciences Discussions*, 7(2).

Valentine DL, Blanton DC, Reeburgh WS, Kastner M (2001). Water column methane oxidation adjacent to an area of active hydrate dissociation, Eel River Basin. *Geochim Cosmochim Acta* 65:2633–2640

Valentine, D. L. (2011). Emerging topics in marine methane biogeochemistry. *Annual review of marine science*, 3, 147-171.

Wilson, R. D., Monaghan, P. H., Osanik, A., Price, L. C., & Rogers, M. A. (1973). Estimate of annual input of petroleum to marine environment from natural marine seepage: ABSTRACT. *AAPG Bulletin*, 57(9), 1840-1840.

Wilson, R. D., Monaghan, P. H., Osanik, A., Price, L. C., & Rogers, M. A. (1974). Natural marine oil seepage. *Science*, 184(4139), 857-865.

Figures and Tables:

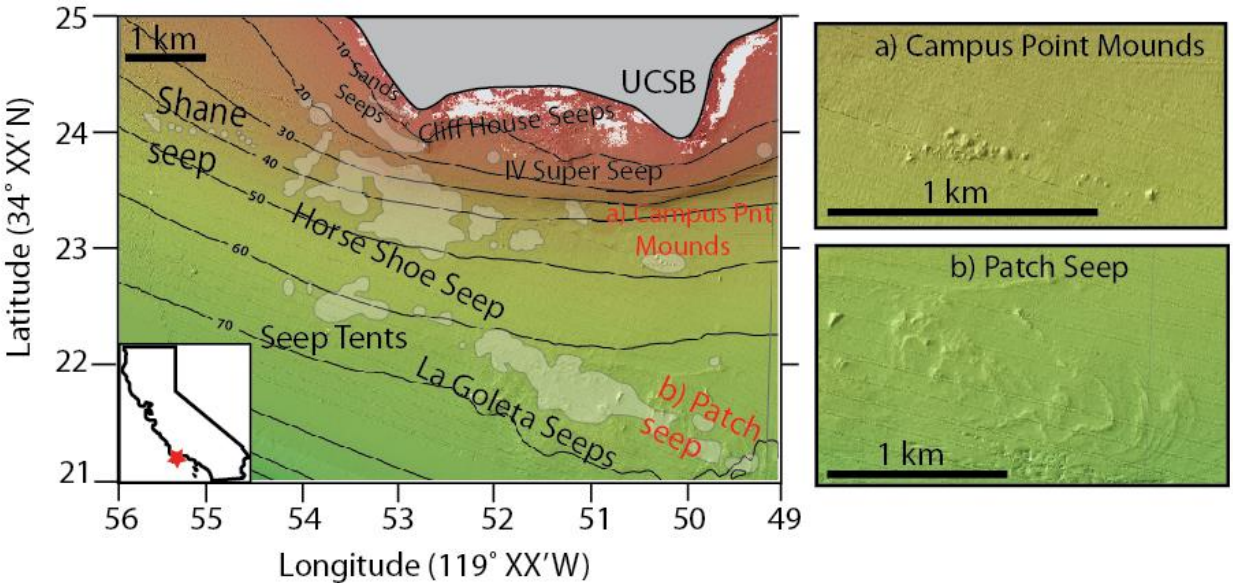

Figure 1. Map of Coal Oil Point seep field with CPM and Patch seep highlighted in red. Contour lines are shown in meters. Panel (a) and (b) show bathymetric data for Campus Point Mounds and Patch Seep from Dartnell et al. (2014).

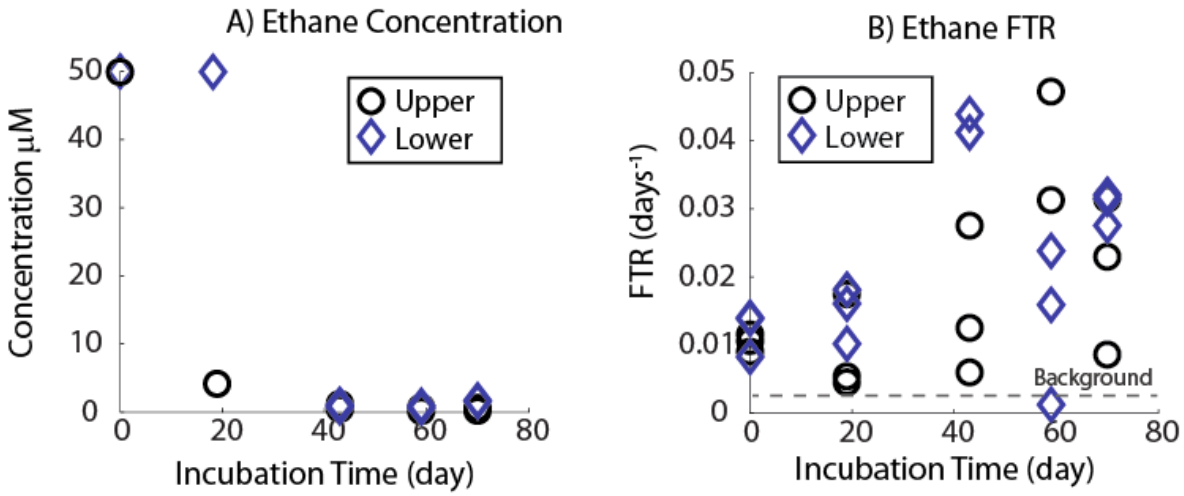

Figure 2. CPM anoxic slurry experiments with long-term incubations, showing ethane concentration (left panel) and fractional turnover rate (FTR, right panel) of upper (circles) and lower section (diamonds) samples. Background rate is shown with dotted line, as determined for kill controls.

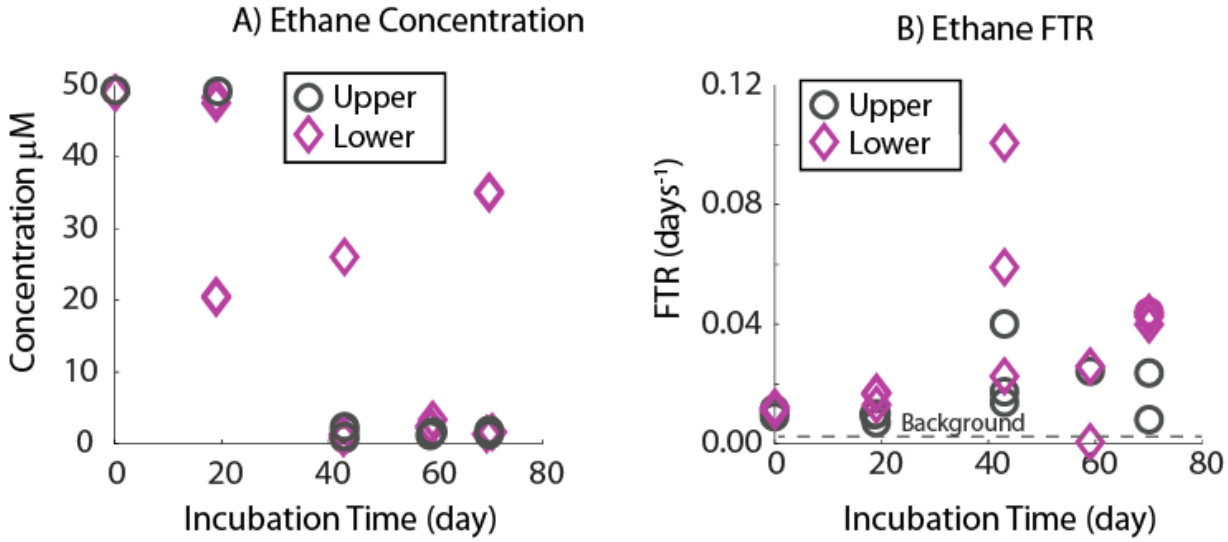

Figure 3. Patch seep anoxic slurry experiments with long-term incubations, showing ethane concentration (left panel) and fractional turnover rate (FTR, right panel) of upper (circles) and lower section (diamonds) samples. Background rate is shown with dotted line, as determined for kill controls.

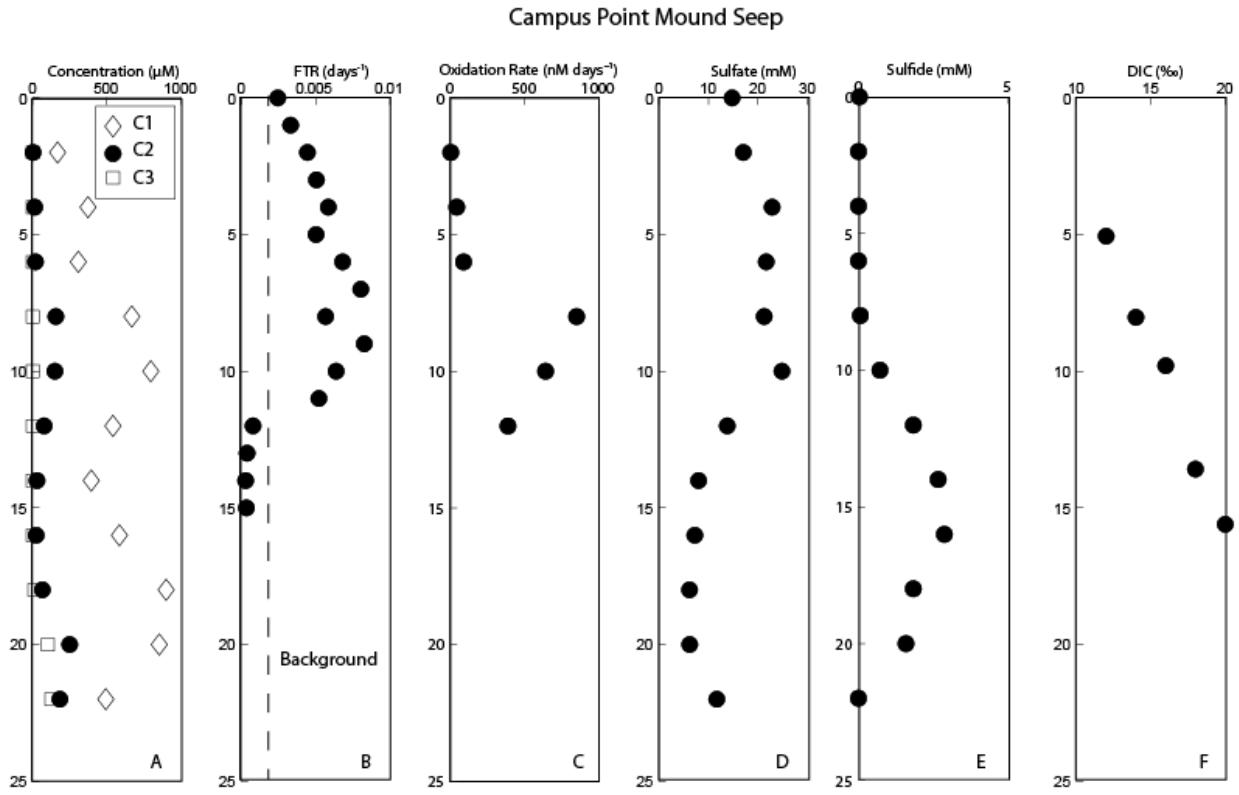

Figure 4. Core depth profiles from CPM: (A) concentration of methane (C1, diamonds), ethane (C2, circles), and propane (C3, squares), (B) fractional turnover rate (FTR), (C) oxidation rate, (D) sulfate concentration, (E) sulfide concentration, (F) δ^{13}C dissolved inorganic carbon.

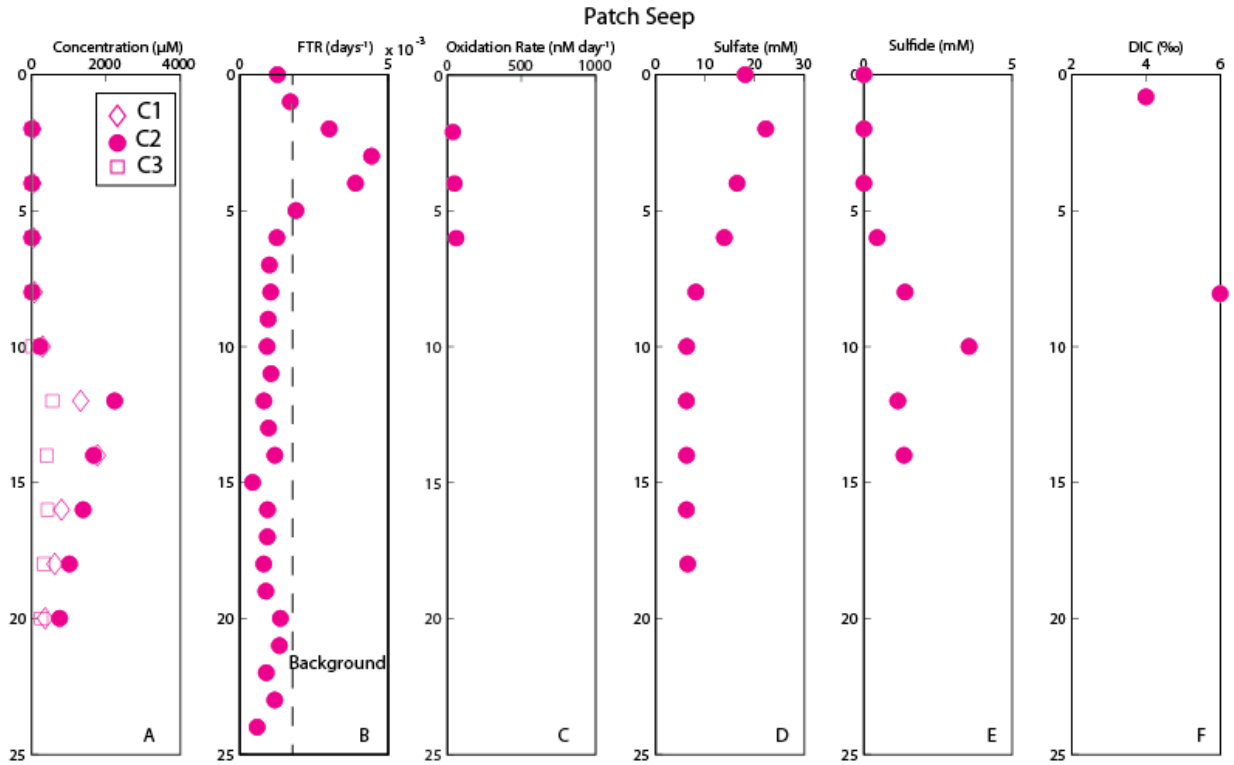

Figure 5. Sediment depth profiles from Patch seep: (A) concentration of methane (C1), ethane (C2), and propane (C3), (B) fractional turnover rate (FTR) for ethane, (C) ethane oxidation rate, (D) dissolved sulfate concentration in the pore fluid, (E) dissolved sulfide concentration in the pore fluid, (F) $\delta^{13}C$ of dissolved inorganic carbon .

Table 1. Sampling Location

Seep Name	**Location (Lat/Long)**	**Depth**	**Area**[a] (m^2)	**Zone of high [SO_4]**	**Sediment Density**	**C2 Oxidation**
CPM	34.392 -119.847	48 m	1000	0-10 cm	1.3 g/mL	2 µM day^{-1} and
Patch	34.364 -119.827	70 m	3000	0-8 cm	1.2 g/mL	0.012 µM day^{-1}

[a] Area estimated from sonar images from Leifer et al. 2010

Table 2. Seep Gas Compositions

Sample	**CH_4 (%)**	**CO_2 (%)**	**Ethane (%)**	**Propane (%)**	**n-butane (%)**	**i-butane (%)**
Seep 1	86.6	9.3	2.0	1.5	0.5	0.2
Patch Seep	82.4	7.7	5.9	2.9	0.7	0.4

Acknowledgements: Sampling and experimental efforts were aided by the Captain and crew of the *R/V Atlantis* and expedition leader and crew of the *ROV JASON* during the SEEPS-13 expedition. Georges Paradis conducted stable isotope analyses, Sarah Lensch, Morgan Raven, Katherine Dawson, Matthias Kellerman, and Alex Phillips assisted in sulfate and sulfide analyses, and Frank Kinnaman collected and analyzed seep gas. Funding for this work was provided by National Science Foundation, grant OCE-1155855, to DLV. SDM was funded by a Ford Foundation Predoctoral Fellowship.

Appendix 1.Water Column Incubation of Natural Gas

Seawater samples were collected from two locations off the coast of California far removed from any known hydrocarbon inputs: (CT2) 37.221433°, -122.52216° and (CT3) 36.565133°, -122.199217°. Samples were collected in 160mL serum bottles and incubated with natural gas at concentrations similar to the Deepwater Horizon oil spill under a variety of gas mixtures, either (i) methane (C1) + ethane (C2) + propane (C3), (ii) C1 + C2, (iii) C1 + C3, (iv) C2 only, or (v) C3 only. No headspace was present at the start of the incubations. Bottles were harvested in replicates at each time point by displacing 5 mL of water into a 30mL syringe. The syringe was filled with an additional 10mL of gas and allowed to equilibrate for a minimum of 12 hours. Samples were analyzed on a GC-FID as described in Chapters 3 and 4.

Table 1.
Experimental data from cast CT2 collected on 27-Sept-2013 from a depth of 50 meters. Samples were collected at a temperature of 11.5°C and incubated at 11°C.

	C1+C2		**C1+C3**		**C2**	**C3**
Incubation Time (days)	**C1 (µM)**	**C2 (µM)**	**C1 (µM)**	**C3 (µM)**	**C2 (µM)**	**C3 (µM)**
0 [a]	100	10	100	10	10	10
7	84.26	8.60	84.10	3.11	2.09	8.9
7	72.58	--	89. 21	0.15	0.37	8.1
7	78.33	9.84	79.02	0.15	1.94	9.6
12	75.64	3.38	36.04	3.61	1.15	5.5
12	67.34	2.84	33.66	0.15	0.51	4.6
12	19.67	1.51	49.67	9.94	0.59	6.3
16	32.48	--	44.87	9.78	0.18	2.28
16	91.34	--	93.33	6.12	0.13	2.27
16	--	--	96.82	6.13	3.96	1.75
23	33.35	--	86.94	0.19	3.90	1.74
23	18.24	--	99.19	0.19	2.61	0.37
23	--	--	100	0.15	2.57	0.38
26	--	--	36.93	0.15	0.15	0.46
26	65.45	--	13.47	0.14	--	0.13
26	22.89	--	79.01	0.15	--	--
29	22.75	3.57	83.44	0.14	--	--
29	--	--	86.39	0.18	--	--

(--) Below detection limits of the GC-FID

[a] Incubation time zero (t_0) represents the bottle concentration following injection of a known quantity of gas.

Table 2.
Experimental data from cast CT3 collected on 27-Sept-2013 from a depth of 1000 meters. Samples were collected at 4.8°C and incubated at 5°C.

	C1+C2		C2
Incubation Time (days)	**C1 (µM)**	**C2 (µM)**	**C2 (µM)**
0	100	10	10
7	76.83	4.86	11.23
7	104.65	4.87	2.31
7	47.49	5.97	0.99
12	72.61	1.26	--
12	79.12	15.73	--
12	92.02	0.49	--
16	87.25	0.99	--
16	55.29	1.05	--
16	53.23	--	--
23	64.74	--	--
23	66.53	--	--
23	59.73	--	--
26	15.69	--	--
26	15.13	--	--
26	15.23	--	--
29	85.04	--	--
29	84.22	--	--
29	24.39	--	--
33	1.99	--	--
33	1.99	--	--
33	32.17	--	--
36	33.27	--	--
36	68.44	--	--
36	62.14	--	--

Table 2, Cont.
Experimental data from cast CT3 collected on 27-Sept-2013 from a depth of 1000 meters. Samples were collected at 4.8°C and incubated at 5°C.

	C1+C2+C3		
Incubation Time (days)	**C1 (µM)**	**C2 (µM)**	**C3 (µM)**
0	100	10	10
7	67.30	10.13	1.61
7	150.64	3.32	4.71
7	36.75	0.45	0.64
12	0	--	--
12	68.48	--	--
12	67.65	--	--
16	77.28	--	--
16	76.13	--	--
16	7.81	--	--
23	8.61	--	--
23	14.47	--	--
23	14.30	--	--
26	58.40	--	--
26	54.11	--	--
26	57.59	--	--
29	59.44	--	--
29	21.72	--	--
29	19.94	--	--
33	26.76	--	--
33	26.46	--	--
33	60.77	--	--
36	61.55	--	--
36	80.19	--	--
36	18.88	--	--

Table 2, Cont.
Experimental data from cast CT3 collected on 27-Sept-2013 from a depth of 1000 meters. Samples were collected at 4.8°C and incubated at 5°C.

	C1+C3		C3
Incubation Time (days)	**C1 (µM)**	**C3 (µM)**	**C3 (µM)**
0	100	10	10
7	66.05	1.06	3.01
7	--	0.58	2.05
7	63.35	0.53	0.93
12	64.98	0.76	0.99
12	67.10	0.065	0.63
12	67.62	0.05	0.72
16	58.83	--	--
16	61.01	--	--
16	9.02	--	0.29
23	5.28	--	0.27
23	18.01	--	0.29
23	18.11	--	0.26
26	6.31	--	--
26	6.15	--	--
26	26.47	--	--
29	26.49	--	--
29	93.64	--	--
29	81.25	--	--
33	2.13	--	--
33	2.13	--	--

Appendix 2. Methane Oxidation Rates from the Gulf of Mexico

Seawater samples were collected near the epicenter of the Deepwater Horizon oil spill in August 2012 aboard the R/V Hatteras (Cruise # CH-03-2012-Kessler). Samples were used to quantify *in situ* methane oxidation rates using the tritiated methane tracer method as described in Chapter 3. All samples were incubated in 160 mL serum bottles and injected with 10 µCi (5 Ci/mmol) of tritiated methane for 24 hours. This work was coordinated by John Kessler of University of Rochester. Additional data are accessible by contacting him directly at john.kessler@rochester.edu. Replicate notation 1 & 2 represent duplicate rate measurements, notation 3 & 4 represent duplicates of kill control rate measurements for the same depth. Kill controls were only measured at select locations and treated with a saturated solution of mercuric chloride.

Station	Niskin Bottle	Replicate	DPM	Factional Turnover Rate
1	6	4	44.42	0.00033
1	6	2	102.63	0.00077
1	6	3	50.18	0.00038
1	6	1	93.98	0.00071
1	7	2	59.06	0.00044
1	7	1	51.21	0.00038
1	8	1	68.31	0.00051
1	9	1	2269.9	0.017
1	9	2	55.37	0.00042
1	10	1	68.40	0.00051
1	10	2	57.96	0.00044
1	11	2	80.63	0.00061
1	11	1	88.95	0.00067
1	17	3	50.88	0.00038
1	17	4	47.69	0.00036
1	17	2	43.95	0.00033
1	18	1	65.92	0.00049
1	18	2	76.89	0.00058
1	19	2	63.47	0.00048
1	19	1	86.50	0.00065
1	20	2	67.65	0.00051
1	20	1	73.21	0.00055
1	21	1	119.69	0.00090
1	21	2	94.61	0.00071
1	22	2	101.02	0.00076
1	22	1	279.45	0.0021

1	23	2	62.78	0.00047
1	23	1	61.57	0.00046
1	24	1	16439.25	0.12
1	24	4	74.82	0.00056
1	24	2	2407.31	0.018
1	24	3	83.60	0.00063
3	6	2	143.41	0.0011
3	6	1	167.57	0.0013
3	6	3	52.27	0.00039
3	6	4	48.90	0.00037
3	7	2	77.05	0.00058
3	7	1	216.00	0.0016
3	9	2	70.76	0.00053
3	9	1	60.06	0.00045
3	16	2	133.48	0.0010
3	16	1	110.85	0.00083
3	17	2	159.15	0.0012
3	17	1	144.36	0.0011
3	18	1	87.11	0.00065
3	18	2	81.81	0.00061
3	19	3	51.46	0.00039
3	19	1	96.44	0.00072
3	19	2	117.38	0.00088
3	19	4	52.23	0.00039
3	20	1	73.94	0.00055
3	20	2	63.85	0.00048
3	21	1	81.39	0.00061
3	21	2	65.90	0.00049
3	22	2	79.60	0.00060
3	22	1	65.82	0.00049
3	23	1	753.11	0.0057
3	23	2	166.61	0.0013
3	24	2	2606.25	0.020
3	24	4	51.45	0.00039
3	24	1	2214.42	0.016
3	24	3	56.53	0.00042
4	6	1	56.11	0.00042
4	6	2	94.83	0.00071
4	9	1	59.99	0.00045

4	9	2	62.55	0.00047
4	11	1	95.89	0.00072
4	11		102.67	0.00077
4	18	1	52.50	0.00039
4	18	2	56.42	0.00042
4	20	2	62.92	0.00047
4	20	4	51.47	0.00039
4	20	1	60.65	0.00045
4	20	3	52.01	0.00039
4	21	2	85.74	0.00064
4	21	1	94.76	0.00071
4	23	2	835.90	0.0063
4	23	1	1700.10	0.013
4	24	1	10087.84	0.076
4	24	2	1988.56	0.014
7	6	1	81.85	0.00061
7	6	2	89.55	0.00067
7	6	4	46.05	0.00035
7	6	3	47.46	0.00035
7	7	1	79.30	0.00080
7	7	2	85.48	0.00064
7	8	2	97.11	0.00073
7	8	1	125.59	0.00094
7	9	2	71.94	0.00054
7	9	1	98.32	0.00073
7	11	1	100.01	0.00075
7	11	2	119.97	0.00090
7	17	1	67.83	0.00050
7	17	2	63.25	0.00047
7	18	2	59.99	0.00045
7	18	1	182.54	0.0013
7	19	1	73.06	0.00054
7	19	2	64.18	0.00048
7	20	1	75.58	0.00056
7	20	2	52.80	0.00039
7	21	2	111.43	0.00083
7	21	1	70.54	0.00052
7	22	2	70.04	0.00052
7	22	1	80.97	0.00060

7	23	1	642.39	0.0048
7	23	2	558.75	0.0041
7	23	3	39.25	0.00029
7	23	3	38.10	0.00028
8	6	3	40.06	0.00030
8	6	4	40.92	0.00030
8	6	1	2101.69	0.015
8	6	2	5757.10	0.043
8	7	1	88.94	0.00066
8	7	2	78.21	0.00058
8	8	1	85.36	0.00064
8	8	2	86.47	0.00064
8	9	1	76.67	0.00057
8	9	2	132.38	0.00099
8	10	1	76.65	0.00057
8	10	2	69.52	0.00052
8	11	1	150.94	0.0011
8	11	2	83.80	0.00062
8	18	1	141.02	0.0010
8	18	2	87.56	0.00065
8	20	1	154.89	0.0011
8	20	2	151.69	0.0011
8	21	1	115.75	0.00086
8	21	2	127.77	0.00093
8	23	1	136.29	0.0010
8	23	2	127.33	0.00095
8	24	3	57.08	0.00042
8	24	4	40.84	0.00030
8	24	1	122.77	0.00092
8	24	2	94.37	0.00070
13	1	2	143.10	0.0010
13	1	1	173.17	0.0013
13	1	2	73.68	0.00055
13	1	1	95.76	0.00071
13	1	2	78.81	0.00059
13	1	3	37.40	0.00028
13	1	4	40.80	0.00030
13	1	3	37.08	0.00027
13	1	4	36.30	0.00027

13	1	1	79.95	0.00060
13	6	2	77.57	0.00058
13	6	2	87.26	0.00065
13	6	1	68.96	0.00051
13	6	1	131.86	0.00098
13	6	2	70.82	0.00053
13	6	1	75.82	0.00056
13	8	1	70.91	0.00053
13	8	2	68.18	0.00051
13	8	1	55.03	0.00041
13	8	2	58.60	0.00043
13	9	2	53.86	0.00040
13	9	2	119.13	0.00089
13	9	1	52.07	0.00039
13	9	2	60.16	0.00045
13	9	1	59.13	0.00044
13	9	1	77.24	0.00057
13	11	1	1082.91	0.0081
13	11	2	921.73	0.0069
13	11	1	68.84	0.00051
13	11	2	57.77	0.00043
13	11	1	49.69	0.00037
13	11	2	54.52	0.00040
13	16	1	73.05	0.00054
13	16	1	854.64	0.0064
13	16	2	59.41	0.00044
13	16	1	76.60	0.00057
13	16	2	77.29	0.00058
13	16	2	527.91	0.0039
13	17	1	72.83	0.00054
13	17	1	93.64	0.00070
13	17	2	56.17	0.00042
13	17	2	72.58	0.00054
13	18	1	76.03	0.00057
13	18	2	67.72	0.00050
13	19	1	605.37	0.0045
13	19	2	1253.04	0.0094
13	19	3	36.10	0.00027
13	19	4	37.00	0.00027

13	20	1	976.29	0.0073
13	20	2	1287.49	0.0096
13	21	1	344.42	0.0025
13	21	2	297.28	0.0022
13	21	3	37.48	0.00028
13	21	4	84.97	0.00063
19	1	2	59.10	0.00044
19	1	1	64.85	0.00048
19	8	1	49.51	0.00037
19	8	2	47.69	0.00035
19	9	1	50.94	0.00038
19	11	1	50.92	0.00038
19	16	1	57.30	0.00043
19	16	2	66.41	0.00049
19	19	1	66.63	0.00050
19	19	2	68.08	0.00051
19	23	1	4715.81	0.035
19	23	2	1306.04	0.0098
20	1	3	38.81	0.00029
20	1	4	37.01	0.00027
20	1	1	43.23	0.00032
20	1	2	51.43	0.00038
20	6	2	57.86	0.00043
20	6	1	51.02	0.00038
20	9	2	63.97	0.00048
20	9	1	57.94	0.00043
20	9	2	53.06	0.00039
20	11	2	55.29	0.00041
20	16	1	53.09	0.00039
20	16	2	55.02	0.00041
20	18	1	57.61	0.00043
20	18	2	49.38	0.00037
21	1	1	47.61	0.00035
21	1	2	50.70	0.00038
21	6	1	62.46	0.00046
21	6	2	63.57	0.00047
21	8	1	46.51	0.00034
21	8	2	122.32	0.00091
21	9	1	60.62	0.00045

21	9	2	59.00	0.00044
21	11	1	56.39	0.00042
21	11	2	51.20	0.00038
21	17	2	47.58	0.00035
21	17	1	48.15	0.00036
21	18	1	63.58	0.00047
21	18	2	63.88	0.00047
21	19	1	54.90	0.00041
21	19	2	53.67	0.00040
21	20	1	77.49	0.00058
21	20	2	63.17	0.00047
21	21	1	79.24	0.00059
21	21	2	68.45	0.00051
21	22	2	72.12	0.00054
21	22	1	74.47	0.00055
21	23	1	78.87	0.00059
21	23	2	81.04	0.00061
21	24	1	2292.67	0.017
21	24	2	1779.11	0.013